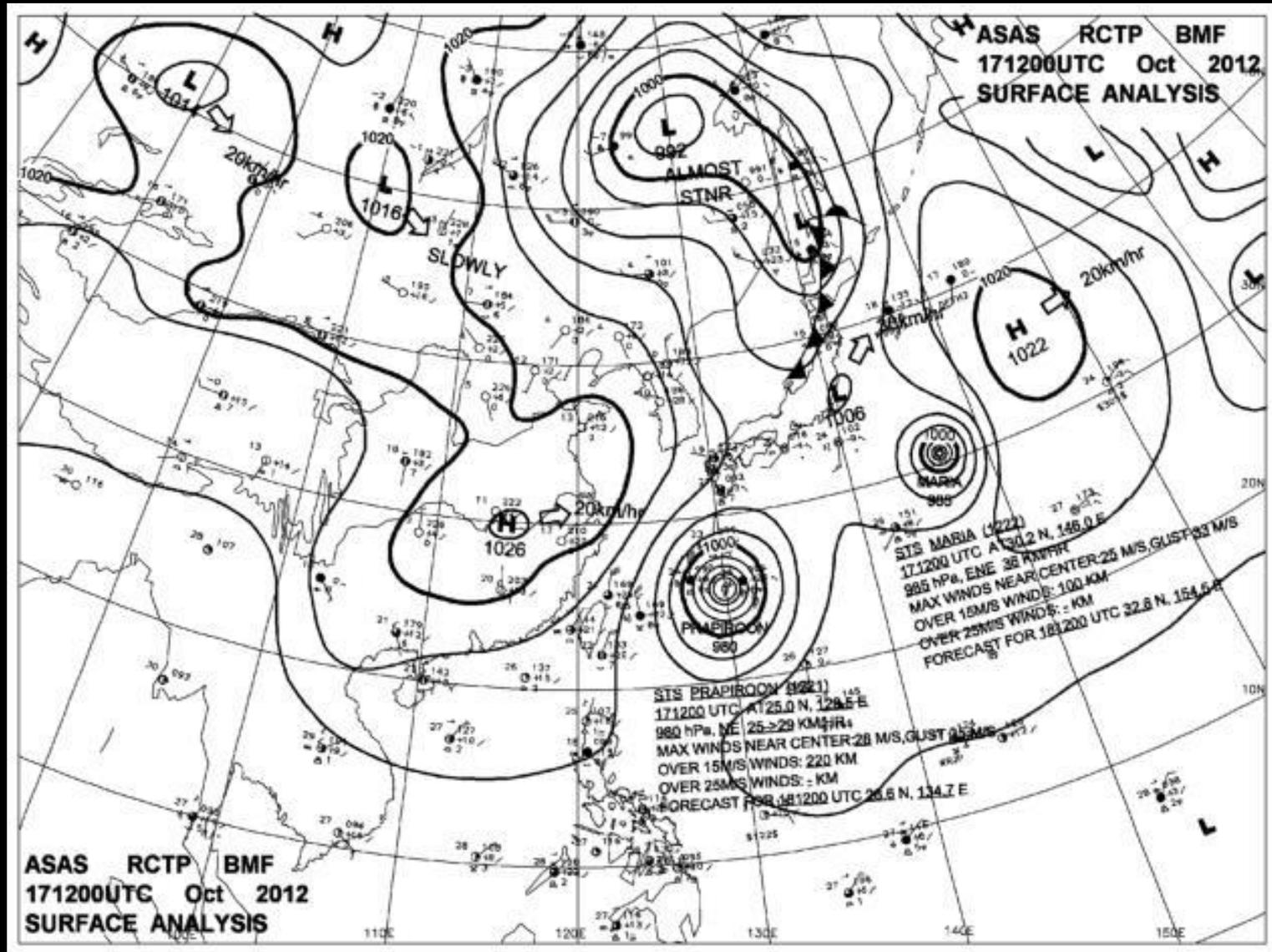


# 第四章:大氣運動-氣壓與風

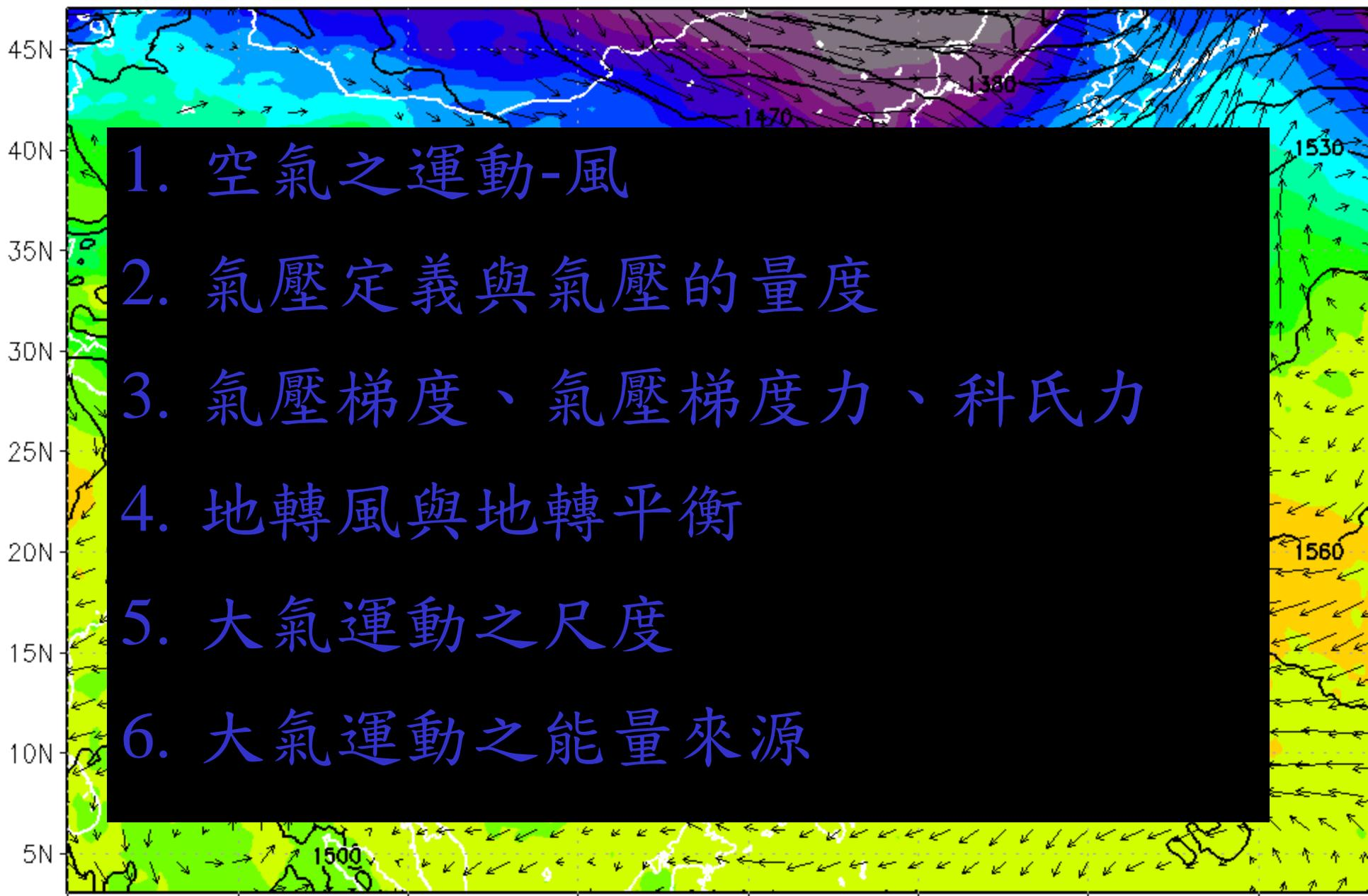


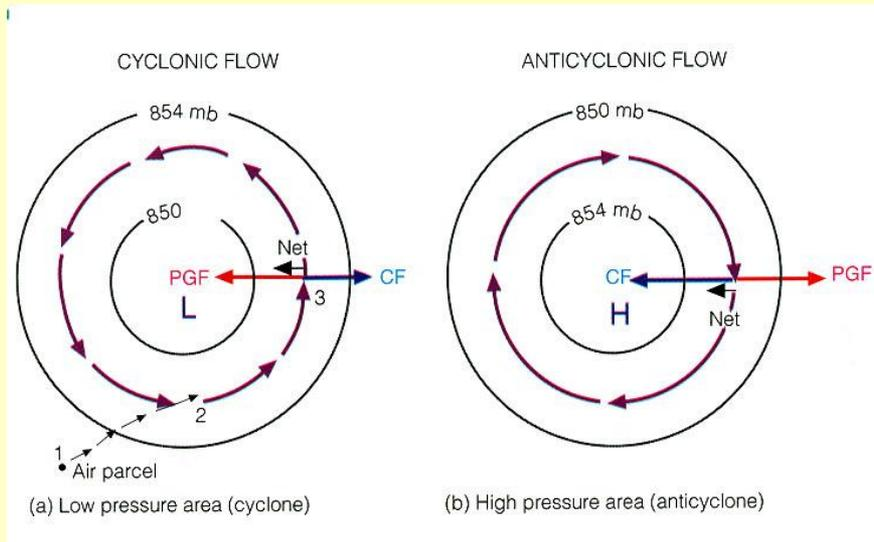
FCST: 12 hr

Valid at: 12 UTC 17 OCT 2012

850 mb wind(vector) / Tmp(shaed)

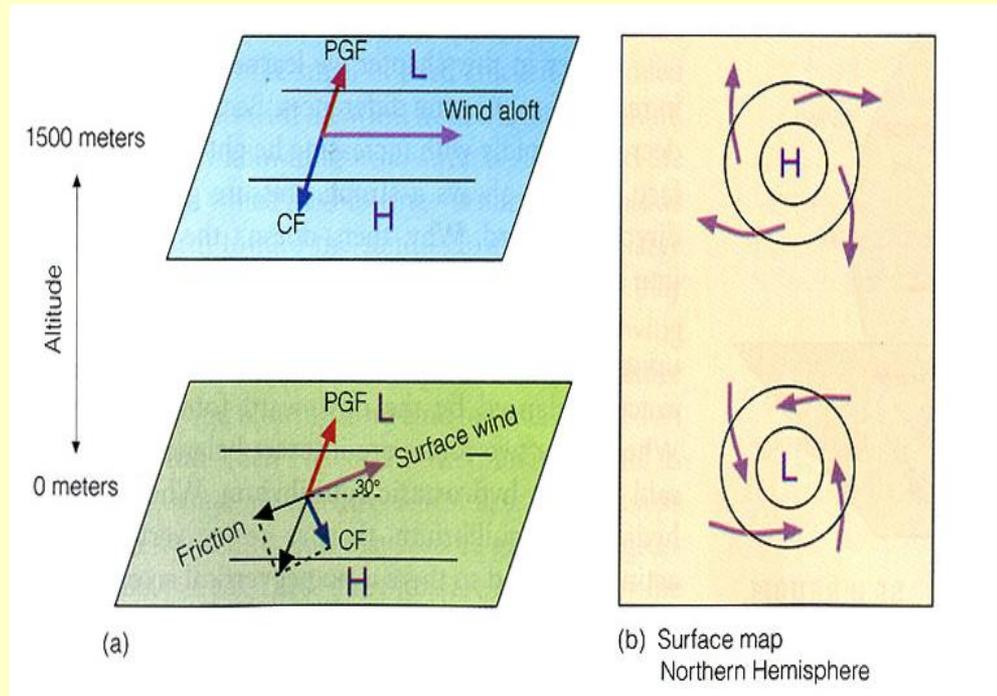
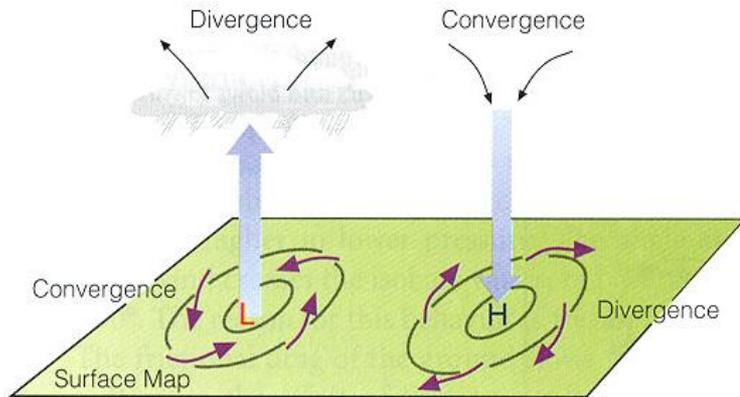
20 LST 17 OCT 2012



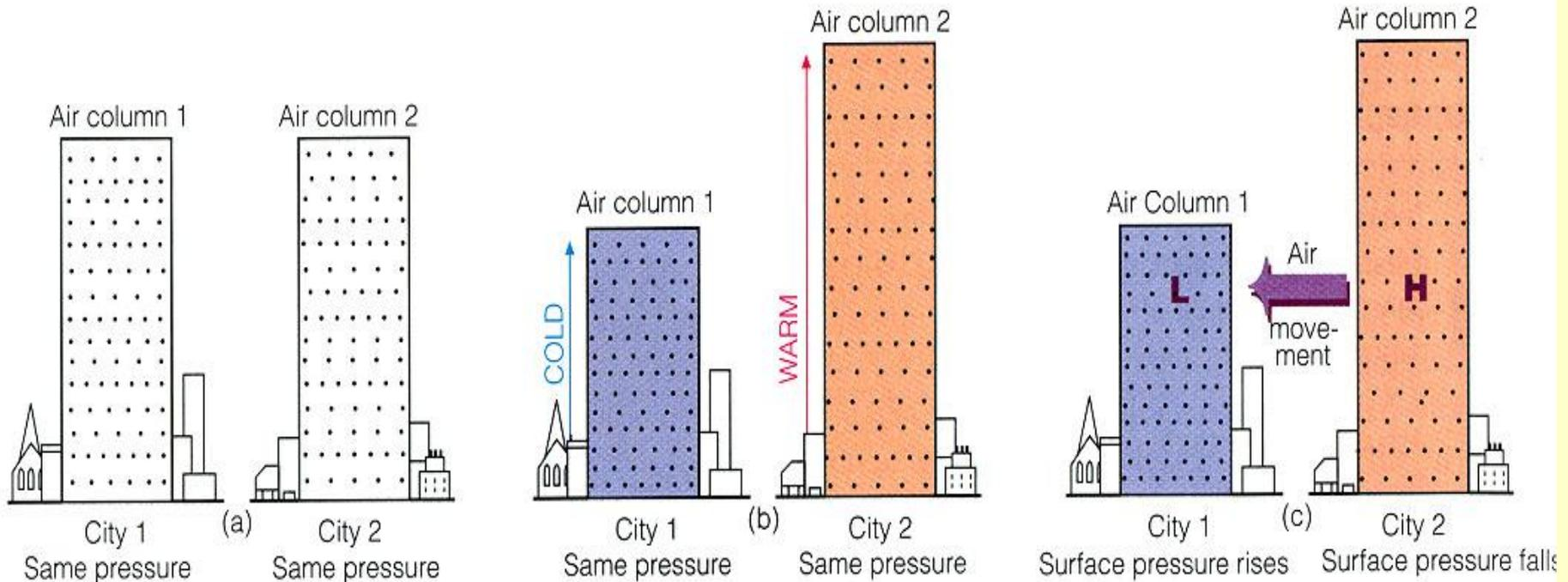


# 氣旋式環流與反 旋式環流

考慮近地表摩擦力所產生之氣流輻合與輻散

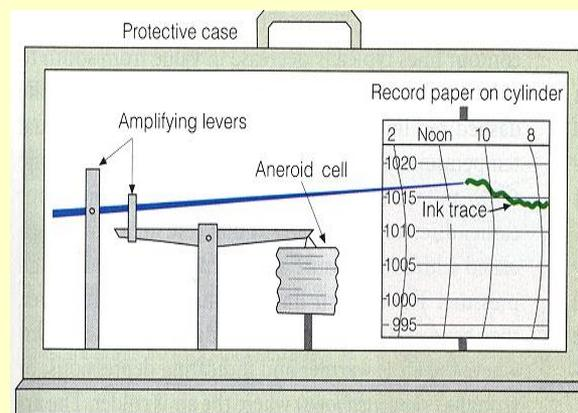
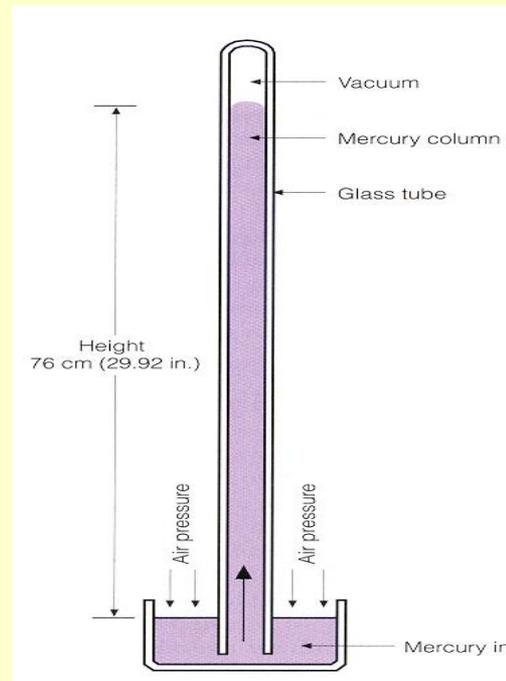
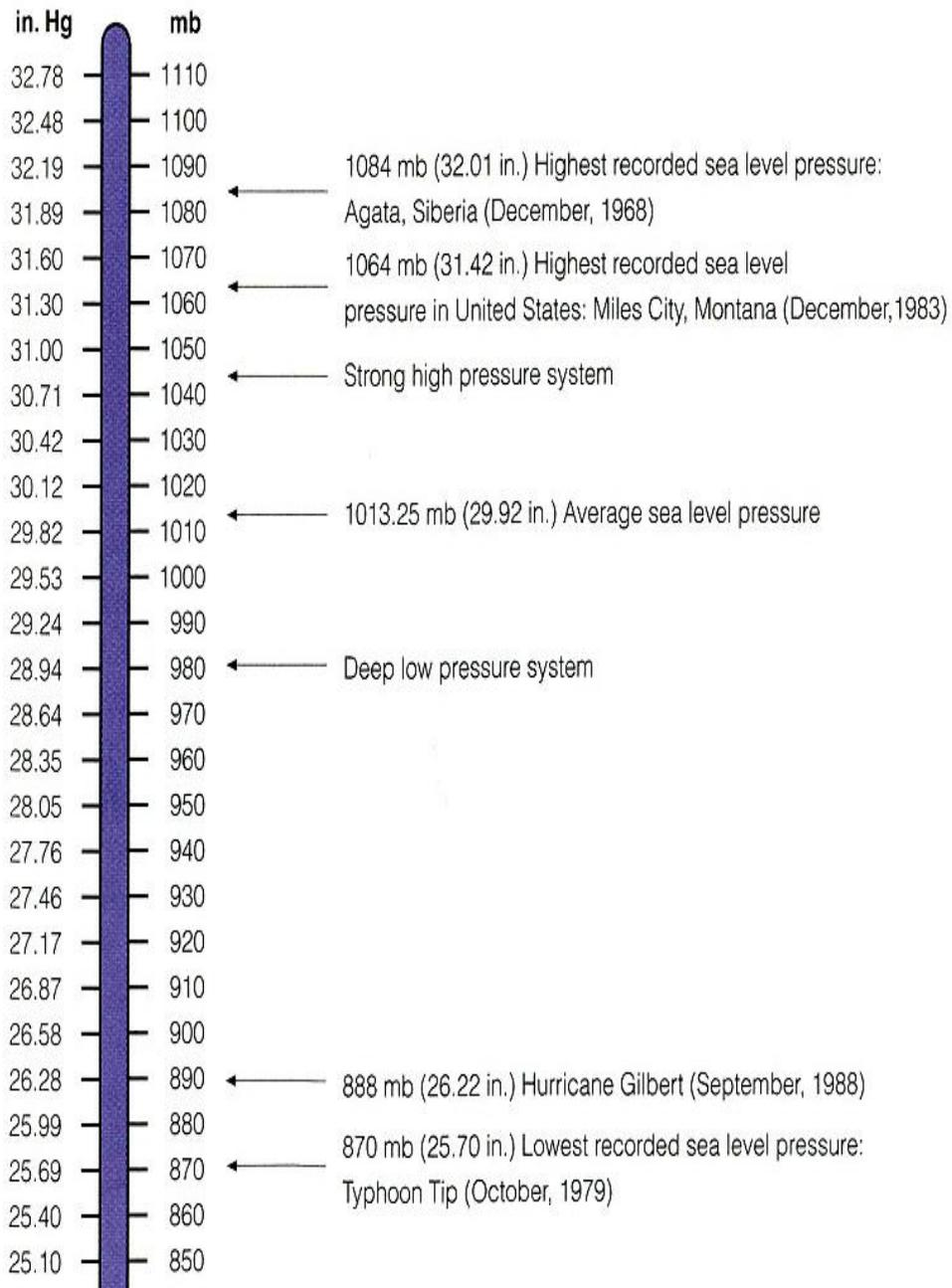


# 氣壓與溫度

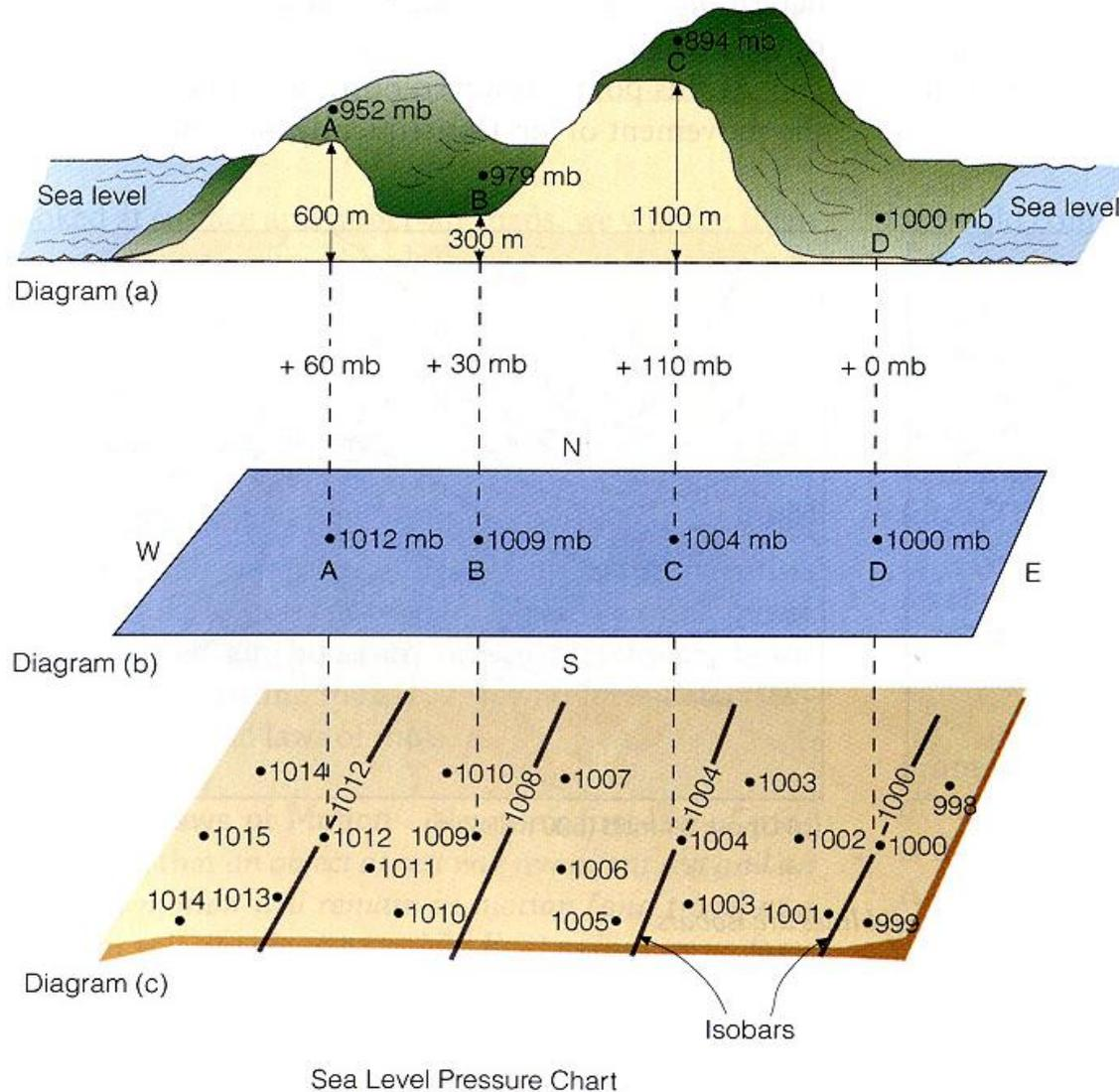


具有相同氣壓的冷暖氣柱，冷氣柱較暖氣柱為短，因而冷氣柱上方為低壓，暖氣柱上方為高壓，氣壓差異造成一股將高壓空氣帶往低壓的力，所以暖氣柱地面氣壓下降，冷氣柱地面氣壓上升。

# 氣壓的度量;水銀氣壓計



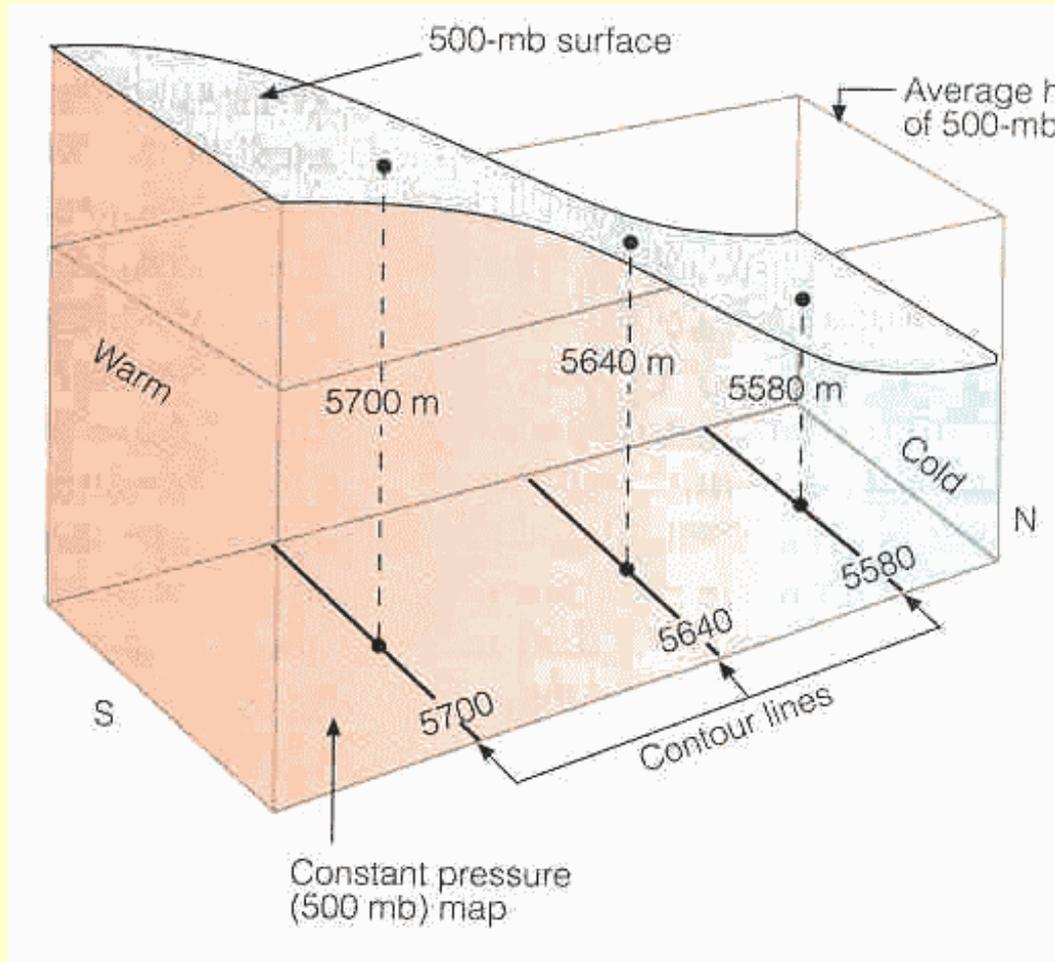
## 地面天氣圖；等壓線



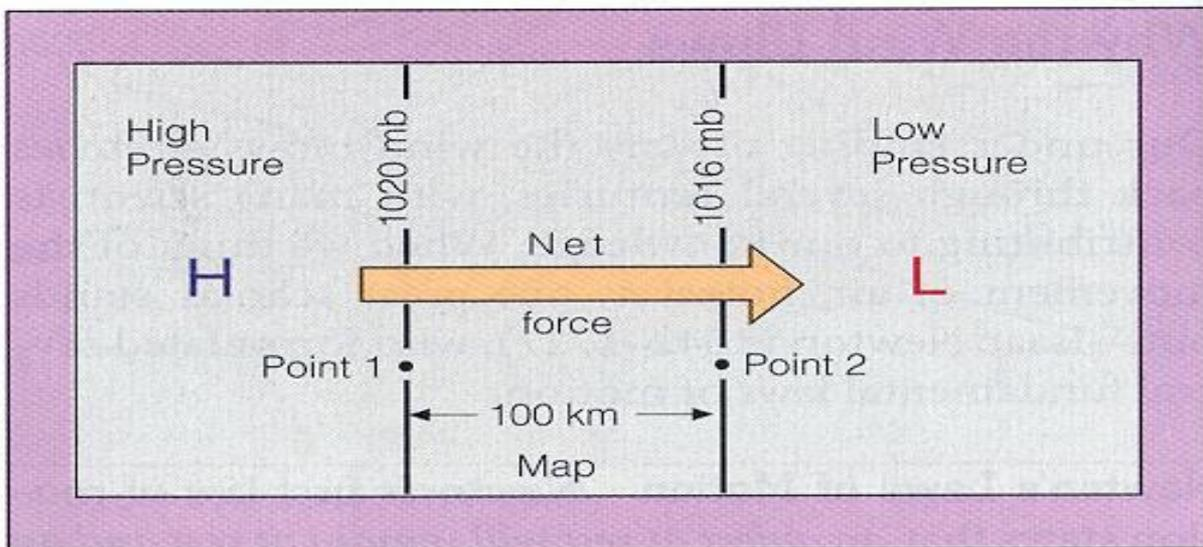
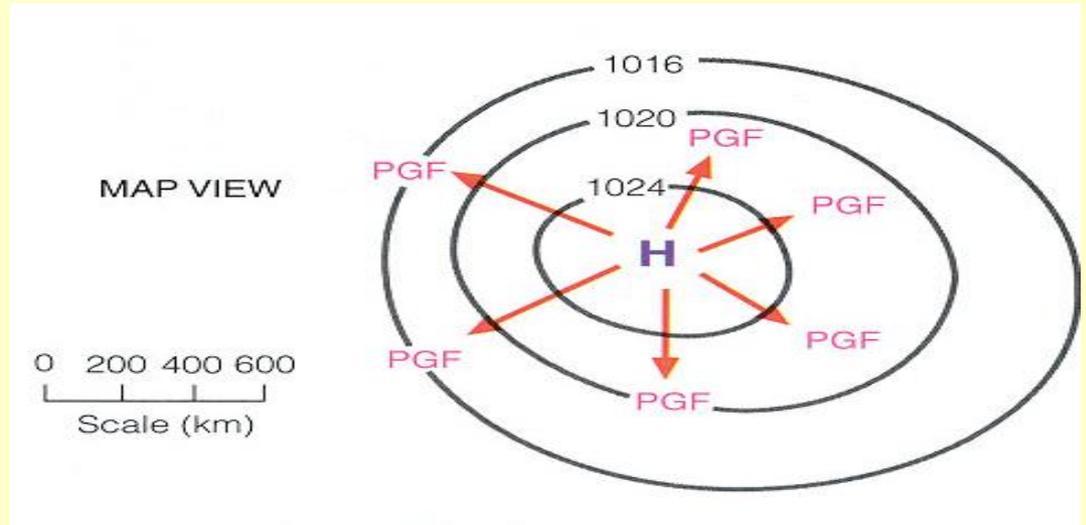
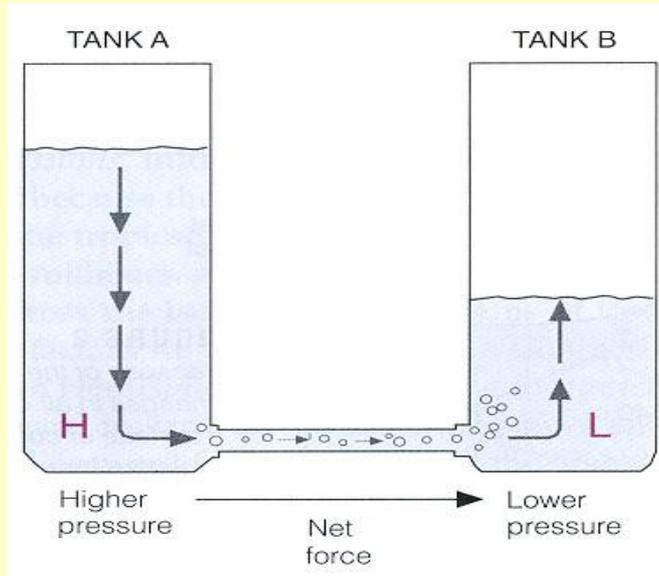
(a) 四個不同海平面高度之城市之測站氣壓(station pressure)，(b) 這四個城市之海平面氣壓(sea level pressure)，(c) 以4 mb為間距之等壓線(isobars)分佈。

**1mb ~ 10m**

# 500hPa 高空天氣圖

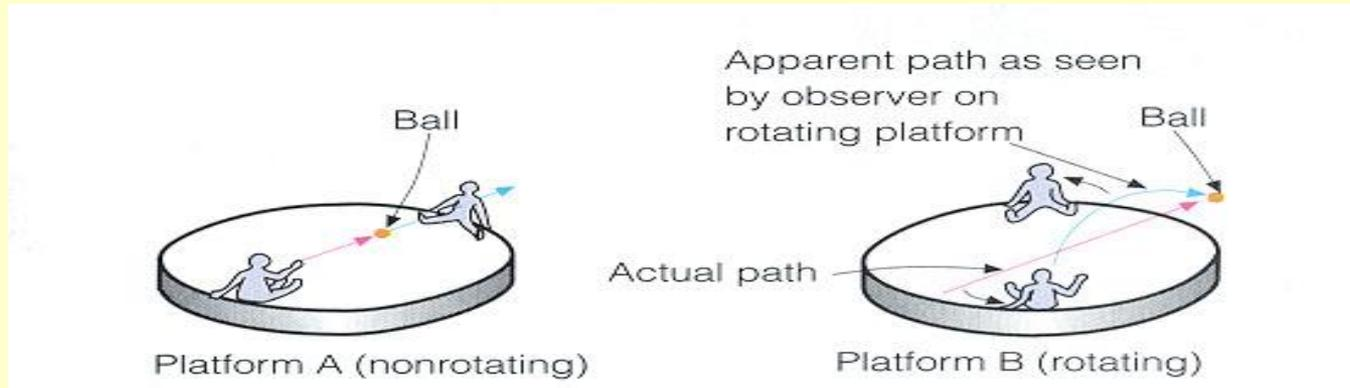


# 氣壓梯度與氣壓梯度力

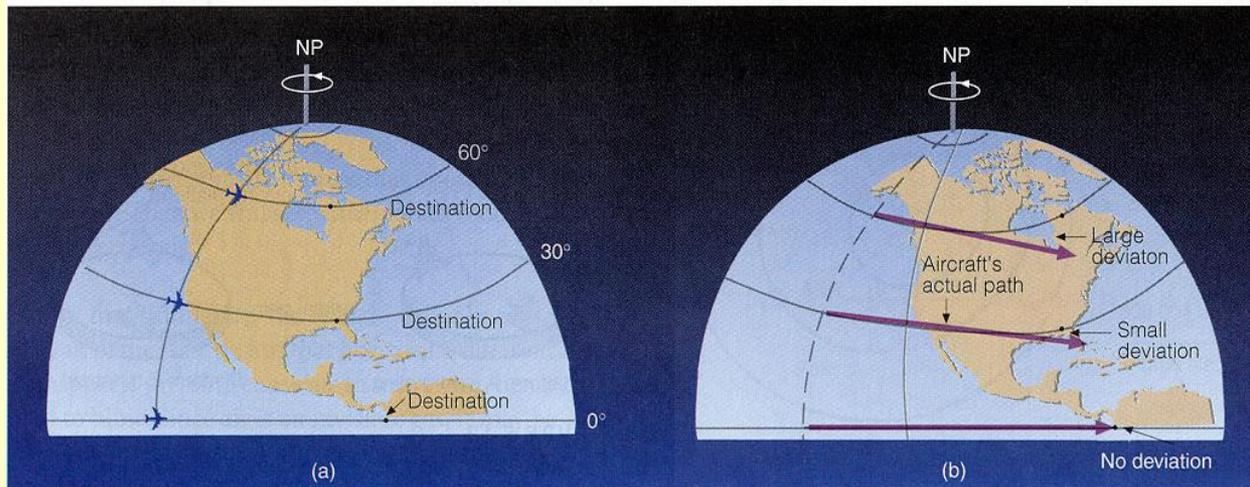


等壓線越密集，氣壓梯度越大，氣壓梯度力也越大。紅色箭頭表示力的大小，並由高壓指向低壓。氣壓梯度力造成風(空氣的移動)。

# 地球自轉與科氏力



未旋轉轉台上丟出的球呈直線運動,在逆鐘向旋轉轉台上,直線丟出的球其運動路徑在轉台上觀察員看來持續向右偏移。除了赤道以外的地區,不論向西或向東的物體其路徑都會受地球旋轉的影響產生偏移。此偏移(科氏力)最大在兩極,到赤道減為零。科氏力的大小與地球旋轉速度、所在緯度、以及物體移動速度有關。



地球是一個快速轉動的行星

地球轉動角速度

$$\Omega = 2\pi / (23\text{hr}56\text{min}4\text{sec}) = 7.292 \times 10^{-5} \text{s}^{-1}$$

在赤道氣塊運動速度

$$v = R_e \times \Omega = 6370\text{km} \times \Omega = 465 \text{ m/s}$$

Venus 1.8 m/s

Mars 239 m/s

地球上海洋與大氣的運動速度( $\sim 10\text{m/s}$ )相對  
旋轉地球而言相當緩慢

## 靜止物體之旋轉效應

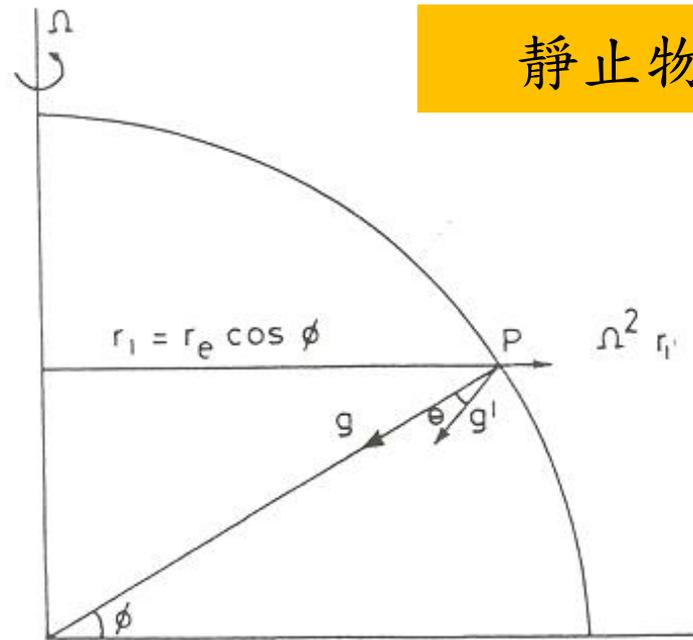


Figure 7.1. Centrifugal acceleration on a particle stationary with respect to the Earth.  $g'$  (effective gravity vector) is the resultant of the centrifugal acceleration and gravity,  $g$ .

- 往外向心加速度(outward centrifugal acceleration)  $\Omega^2 r_1 = 0.034\text{ms}^{-2}$ ,  $g=9.81\text{ms}^{-2}$ ,
- The resultant vector, apparent gravity  $g$  視重力, indicating an angle of  $0.1^\circ$  to the true direction of gravity.
- The local vertical is assumed to be aligned with the resultant gravity vector.

# Coriolis force

Conservation of absolute angular momentum

絕對角動量守恆

$$(\Omega + u/R) R^2 = \{ \Omega + [u+\delta u]/[R+\delta R] \} (R+\delta R)^2$$

$$\delta u = -2\Omega\delta R - (u/R) \delta R$$

in the case of a meridional displacement in which  $\delta R = -\sin\phi\delta y$ , then we have

$$Du/Dt = [-2\Omega \sin\phi + (u/a) \tan\phi] Dy/Dt$$

$$\mathbf{Du/Dt} = -2\Omega\sin\phi\mathbf{v} + (\mathbf{uv/a}) \tan\phi$$

# Coriolis force

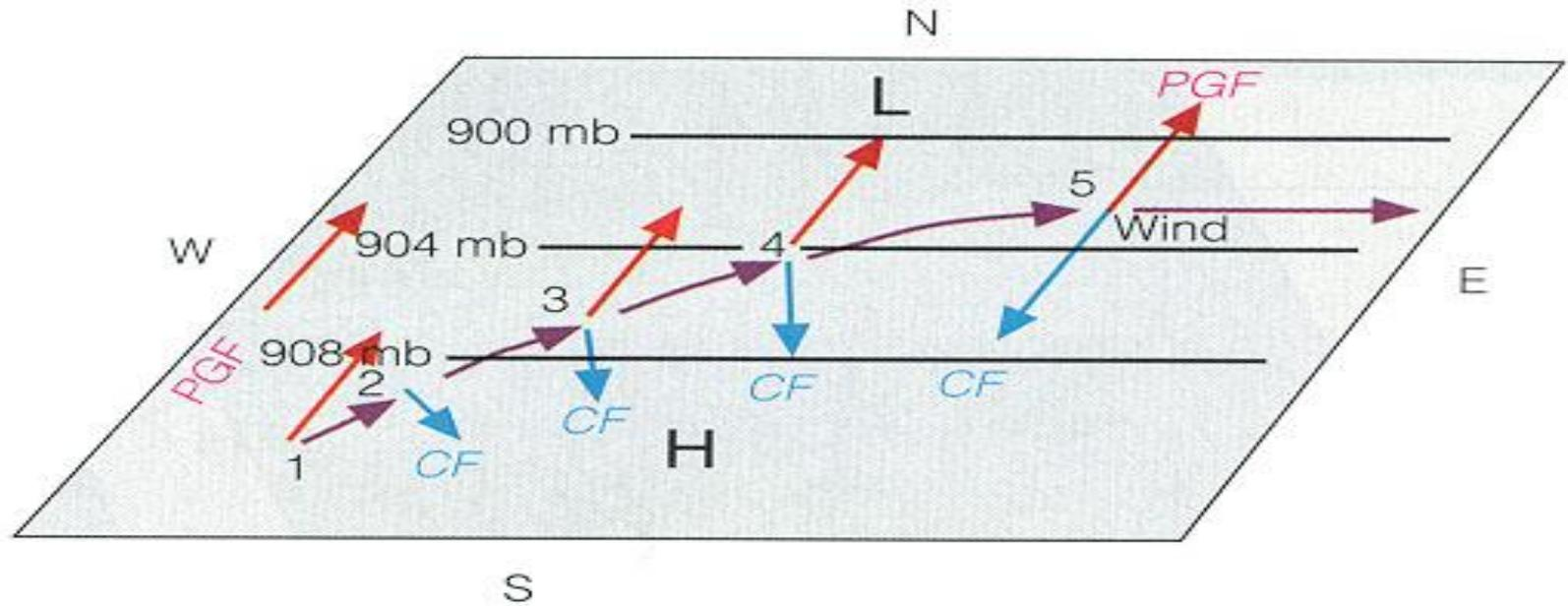
Change of centrifugal force corresponding to a displacement of the object at rest in x-direction:

$$(\Omega + u/R)^2 \mathbf{R} - \Omega^2 \mathbf{R} = 2\Omega u (\mathbf{R}/R) + u^2 (\mathbf{R}/R^2)$$

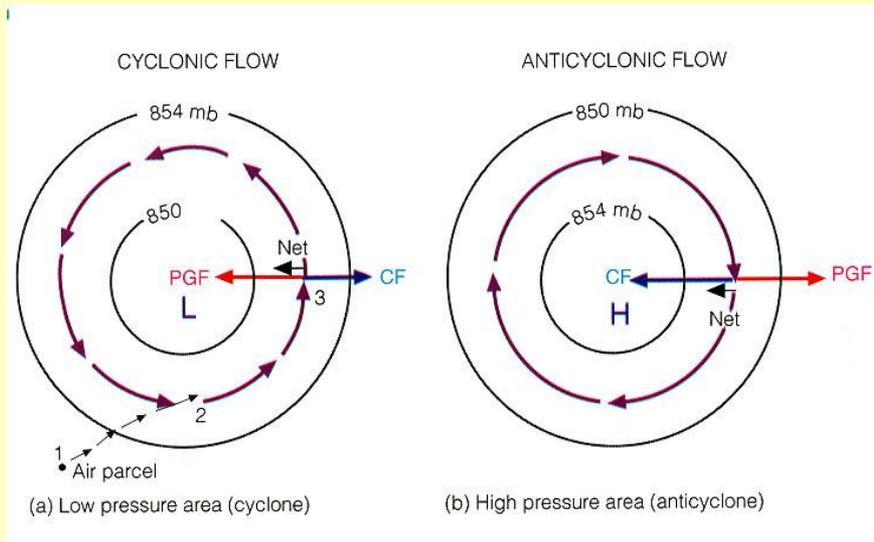
$$\mathbf{Dv/Dt} = -2\Omega \sin\varphi \mathbf{u} - (u^2/a) \tan\varphi$$

$$\mathbf{Dw/Dt} = 2\Omega \cos\varphi \mathbf{u} + u^2/a$$

# 地轉風與地轉平衡

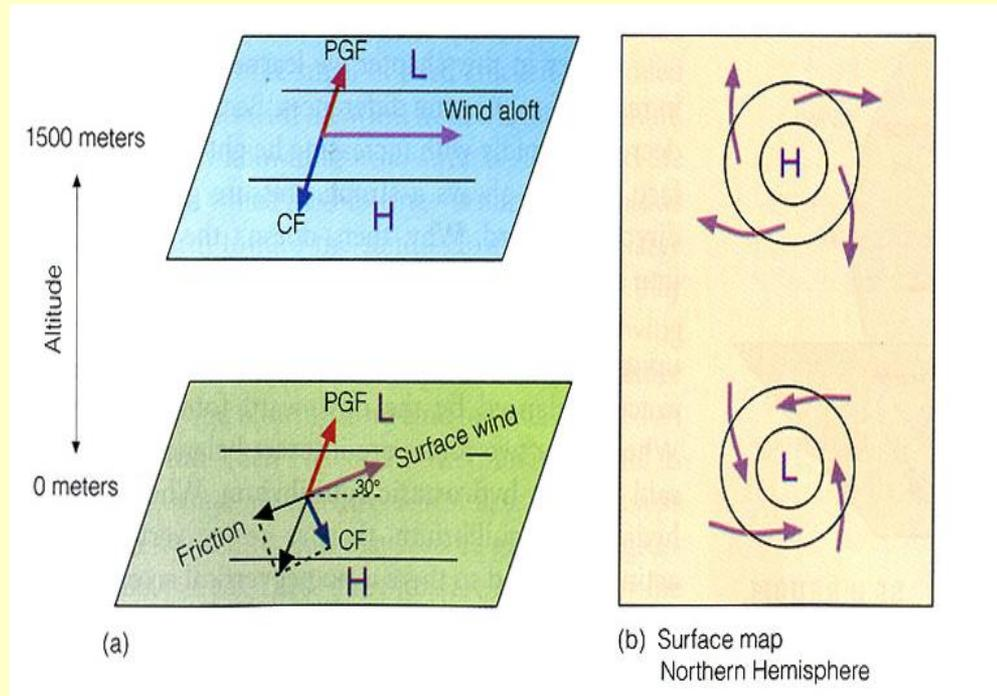
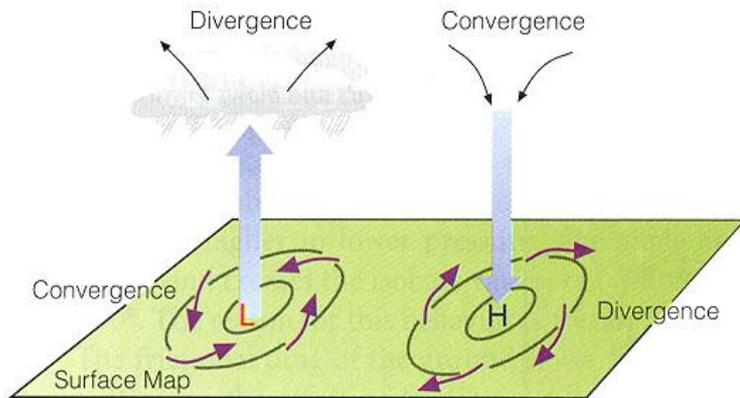


摩擦層之上的空氣，由靜止逐漸加速到一平衡速度，此時風向平行於等壓線，風速大小由氣壓梯度力和科氏力決定，此種平衡狀態稱之為地轉平衡，此平衡風場稱之為地轉風。



# 氣旋式環流與反 旋式環流

考慮近地表摩擦力所產生之氣流輻合與輻散



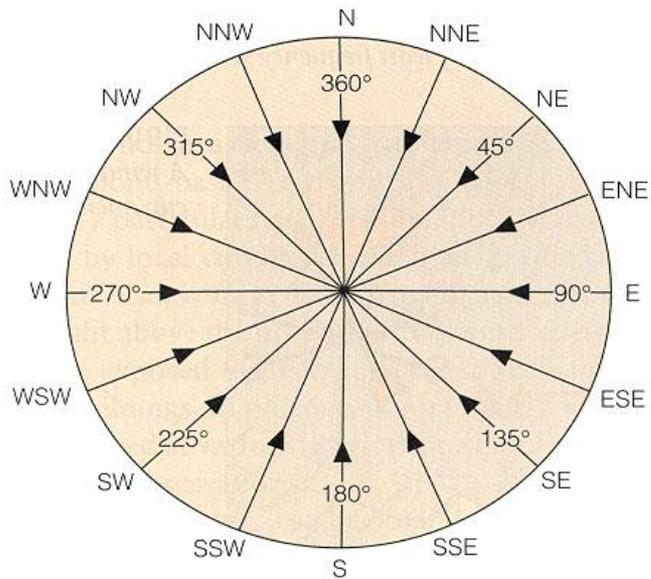


**FIGURE 6.22**

*Wind direction can be expressed in degrees about a circle or as compass points.*

## 風向及風花圖

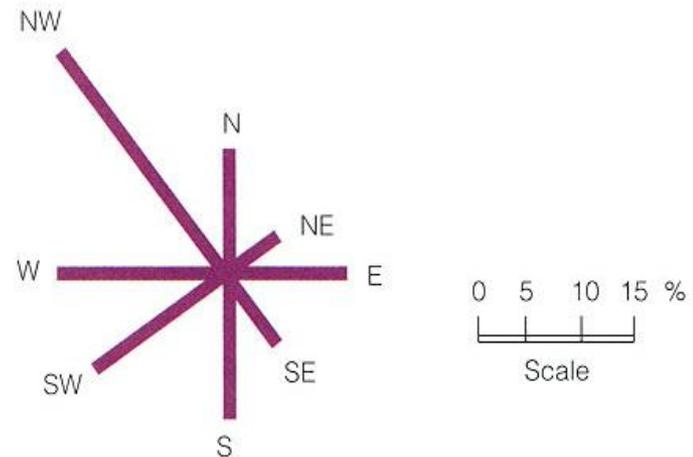


**FIGURE 6.24**

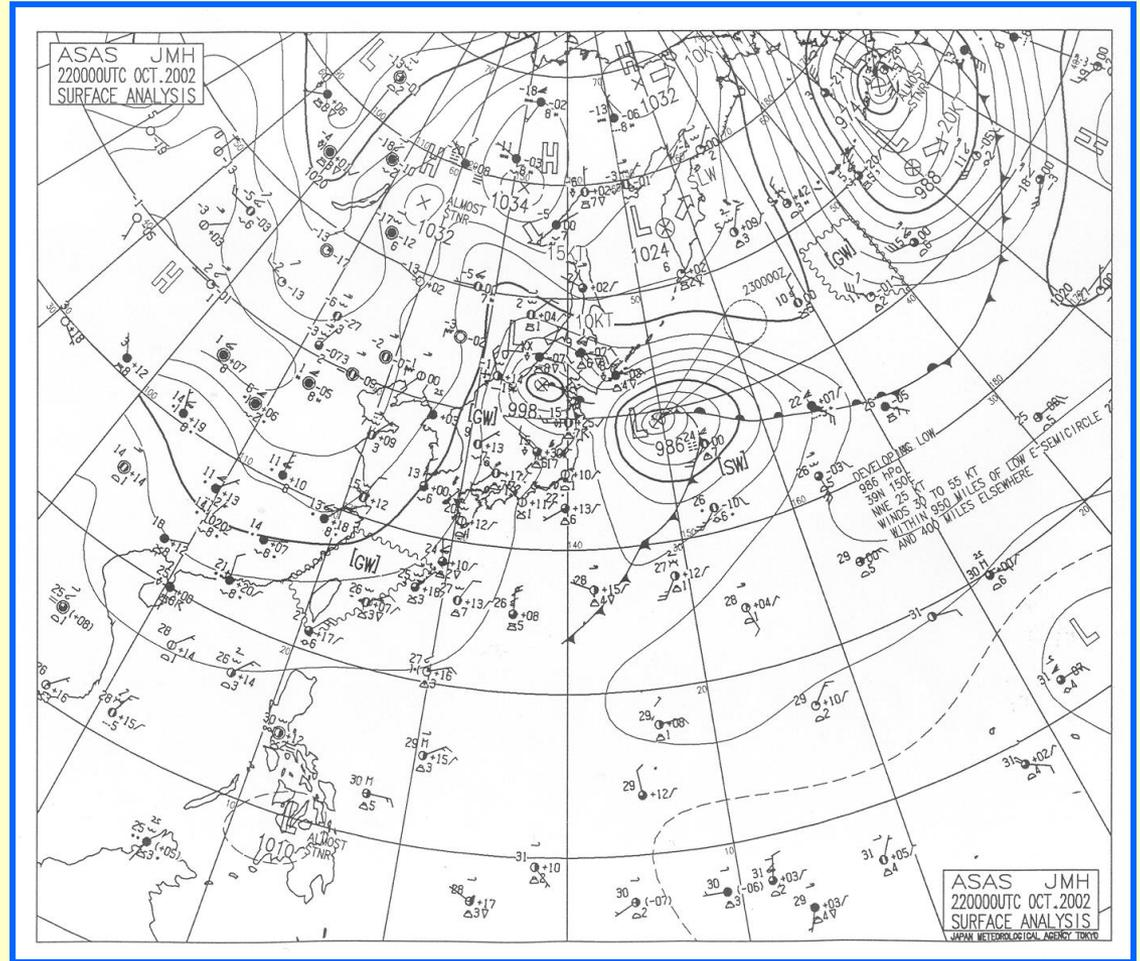
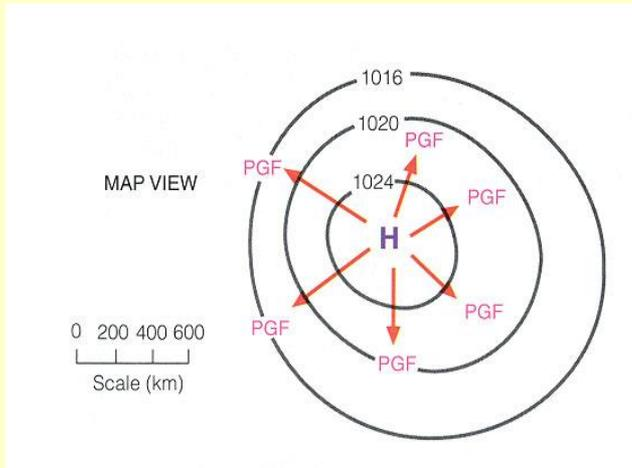
*This wind rose represents the percent of time the wind blew from different directions at a given site during the month of January for the past ten years. The prevailing wind is NW and the wind direction of least frequency is NE.*



**FIGURE 6.26**

*The aerovane (skyvane).*

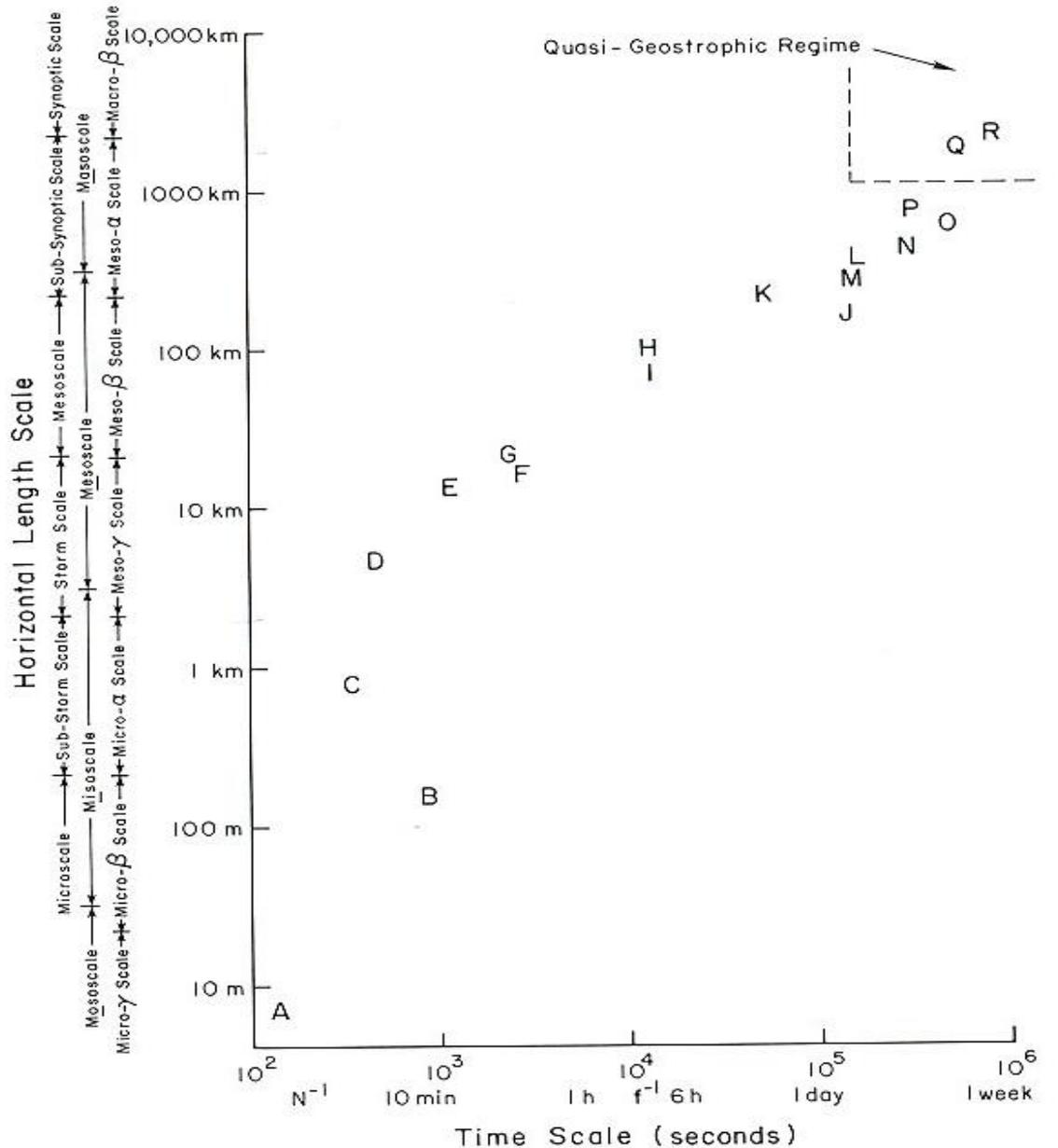
# 氣壓梯度與氣壓梯度力



等壓線越密集，氣壓梯度越大，則氣壓梯度力越強。氣壓梯度力由高壓指向低壓。

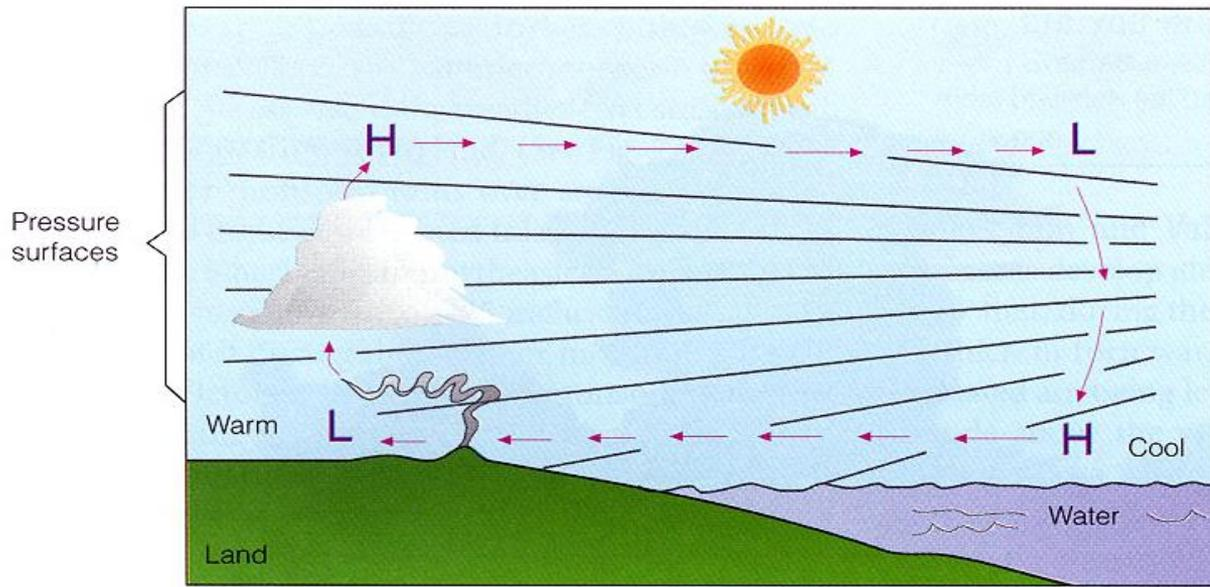
問題:為何低壓中心附近的氣壓梯度較大而高壓中心附近的氣壓梯度較小?

# 大氣運動之尺度

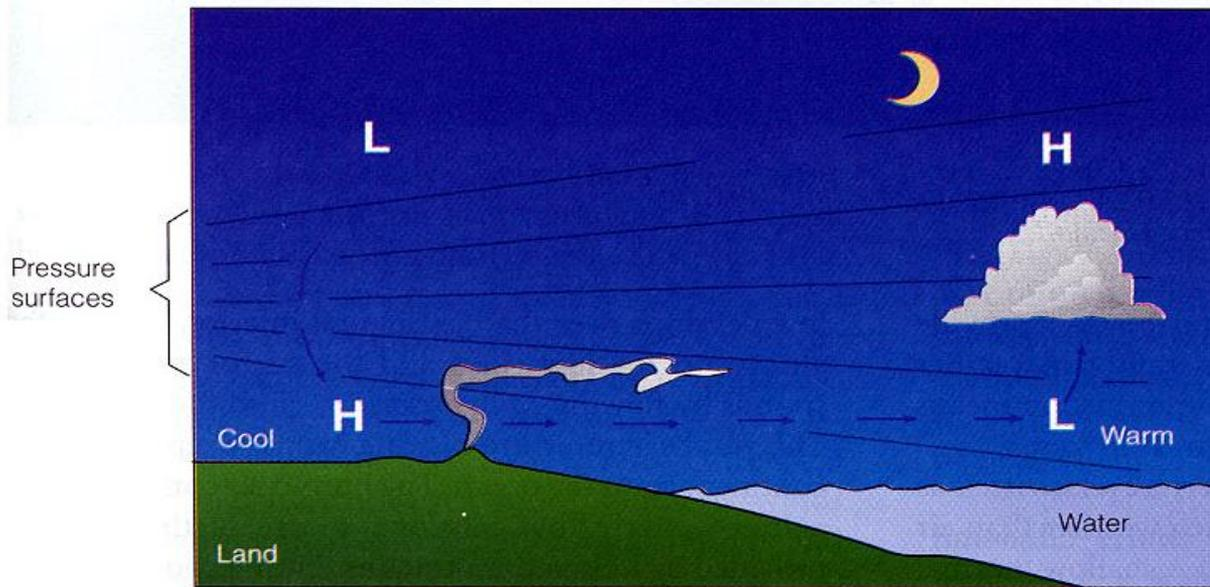


大氣現象依水平空間尺度及時間尺度之分布圖。

- A: 塵暴
- B: 龍捲風和水龍捲
- C: 積雲
- D: 下爆氣流
- E: 陣風鋒面
- F: 中尺度氣旋
- G: 雷暴
- H: 海陸風、山谷風等環流及中尺度高低壓
- I: 雨帶
- J: 海岸鋒
- K: 中尺度對流系統
- L: 低層噴流
- M: 乾線
- N: 熱帶氣旋 (颱風)
- O: 高層噴流
- P: 地面鋒
- Q: 溫帶氣旋與反氣旋
- R: 斜壓西風帶槽脊線

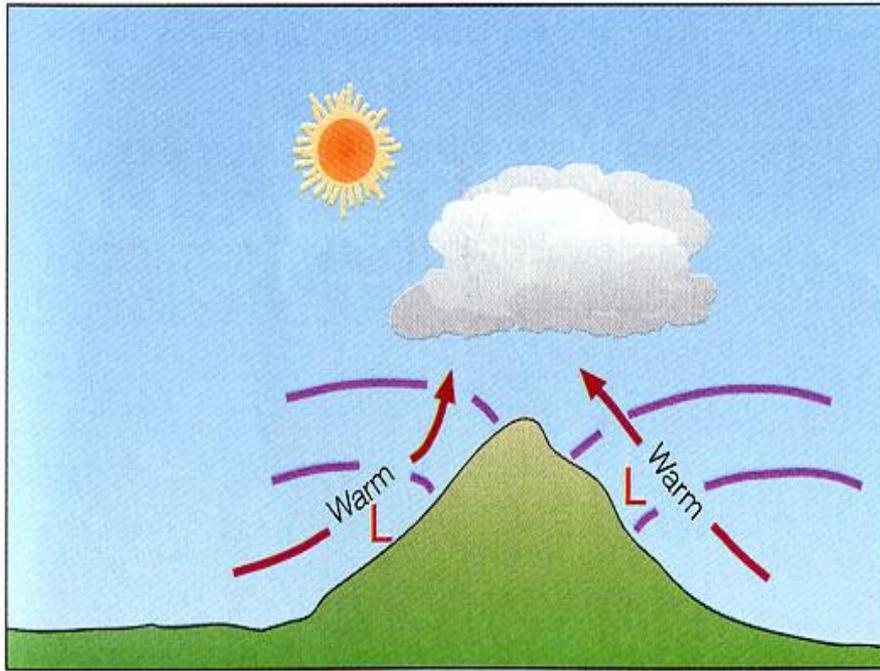


(a) Sea breeze

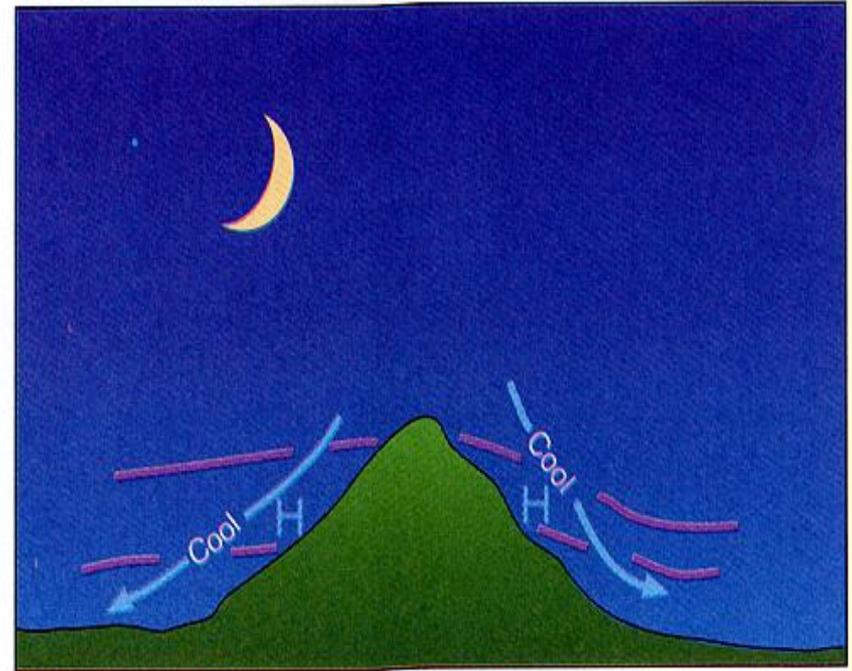


(b) Land breeze

海風和陸風的發展。  
(a) 在地面  
海風由海面吹向  
陸地，  
(b) 陸風  
由陸地吹向海面。



Valley Breeze



Mountain Breeze

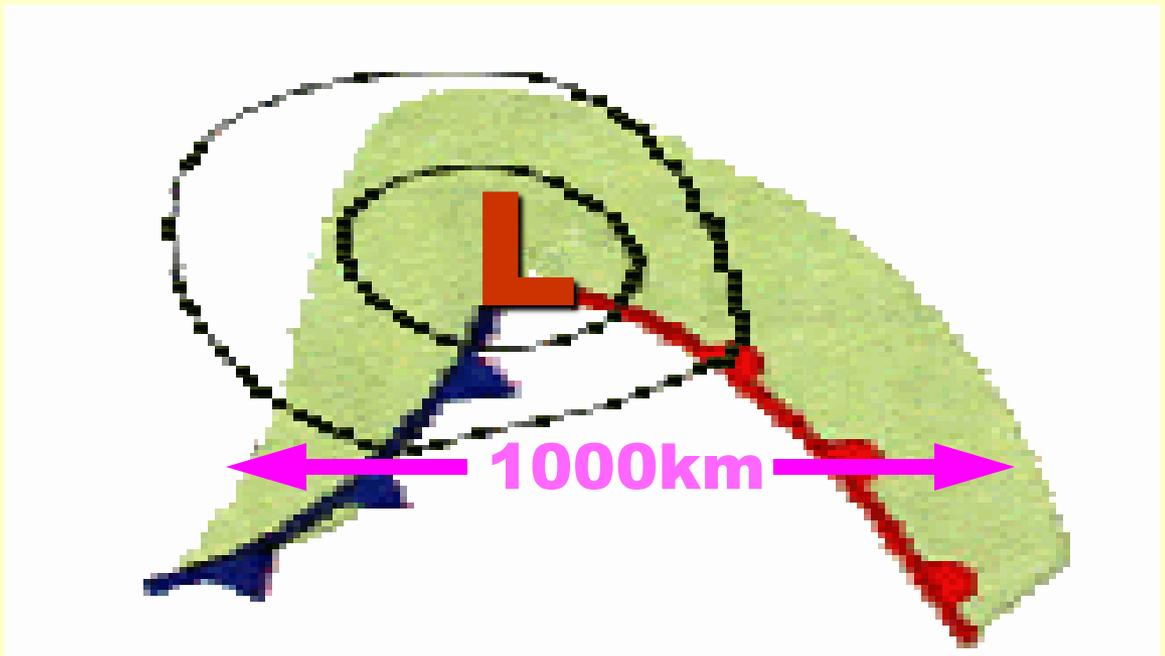
白天吹谷風，晚上吹山風。

## 溫帶氣旋

$$\frac{H}{L} \approx \frac{10\text{km}}{1000\text{km}} \approx \frac{1}{100}$$

$$v \approx 10\text{ms}^{-1}, w \approx 10\text{cms}^{-1}$$

$$\frac{w}{v} \approx \frac{1}{100}$$

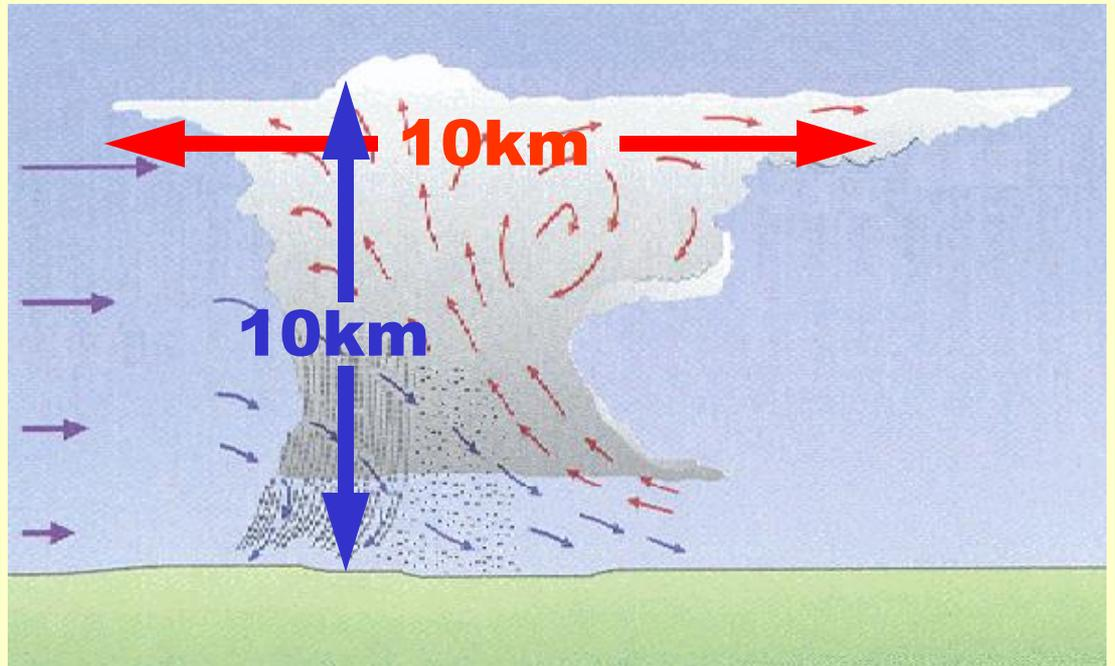


## 雷暴系統

$$\frac{H}{L} \approx \frac{10\text{km}}{10\text{km}} \approx 1$$

$$v \approx 10 \sim 20\text{ms}^{-1}, w \approx 10 \sim 20\text{ms}^{-1}$$

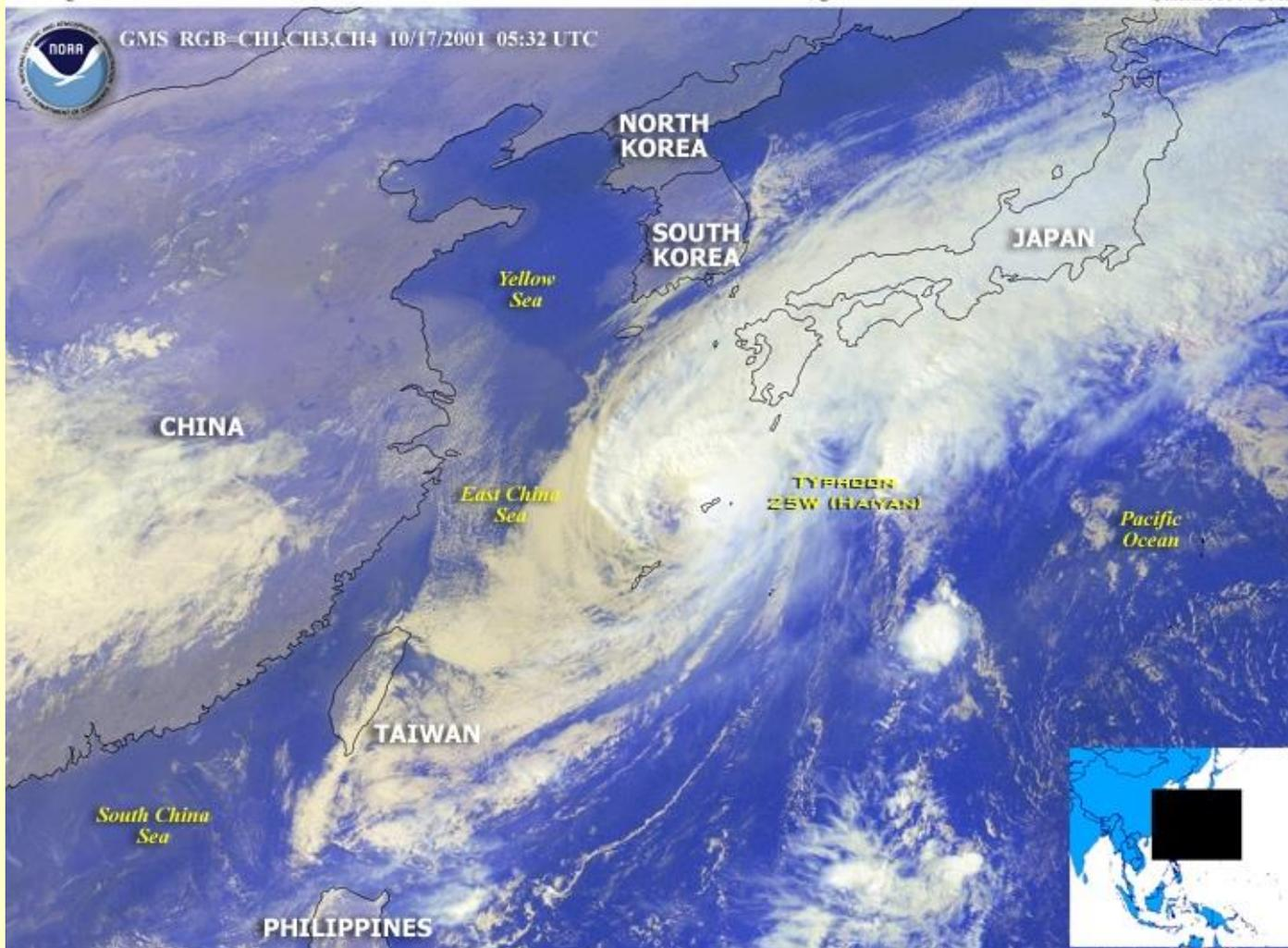
$$\frac{w}{v} \approx 1$$



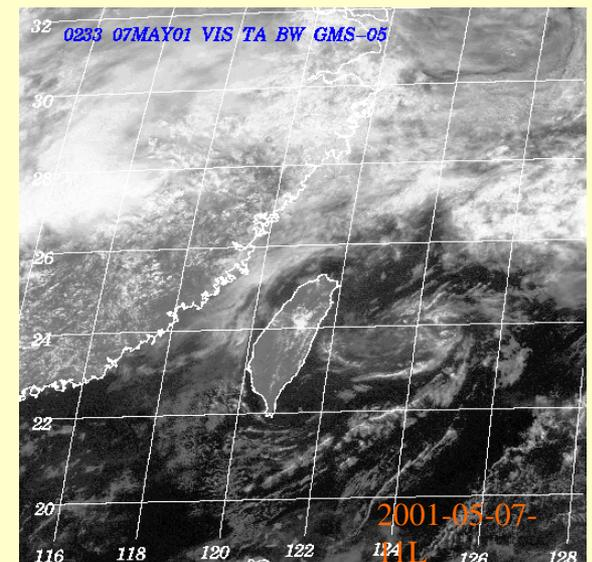
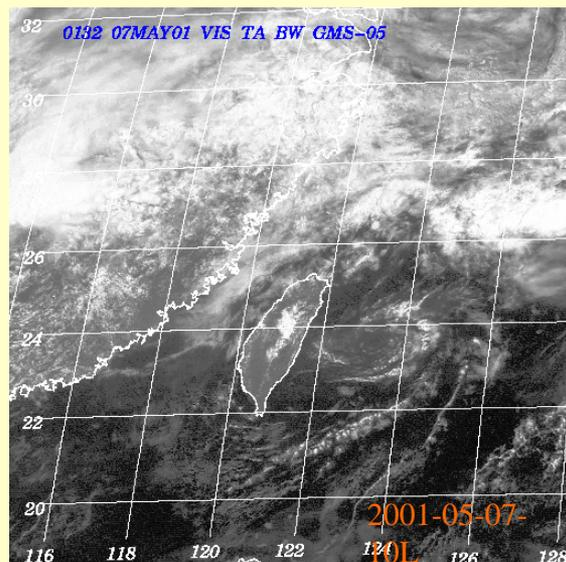
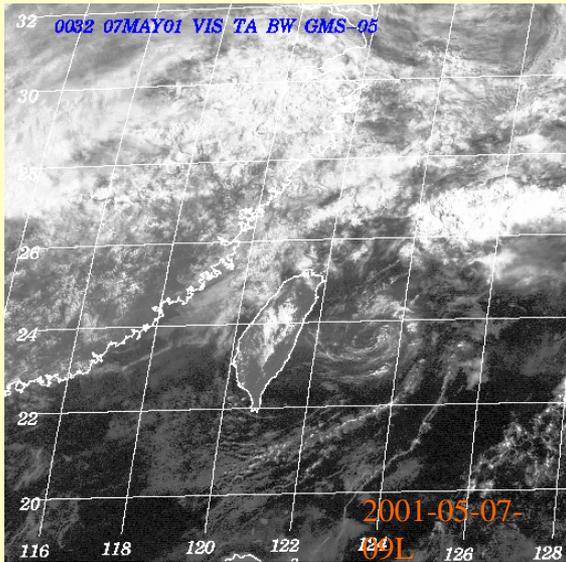
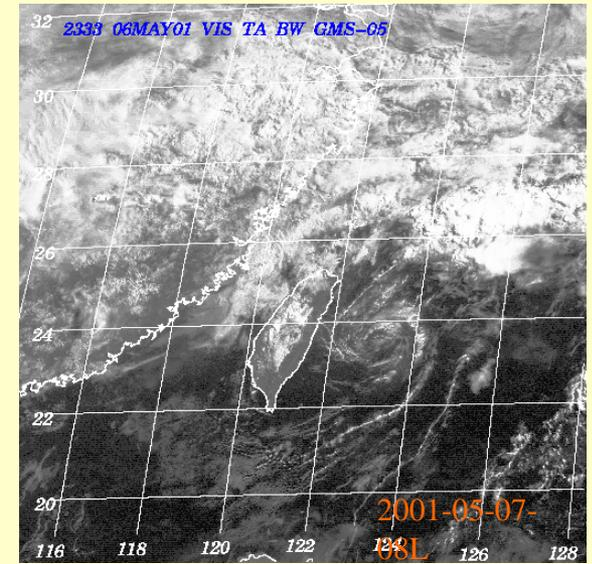
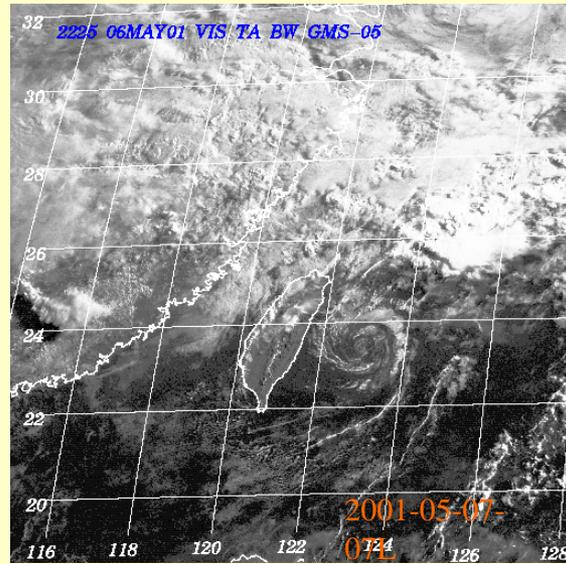
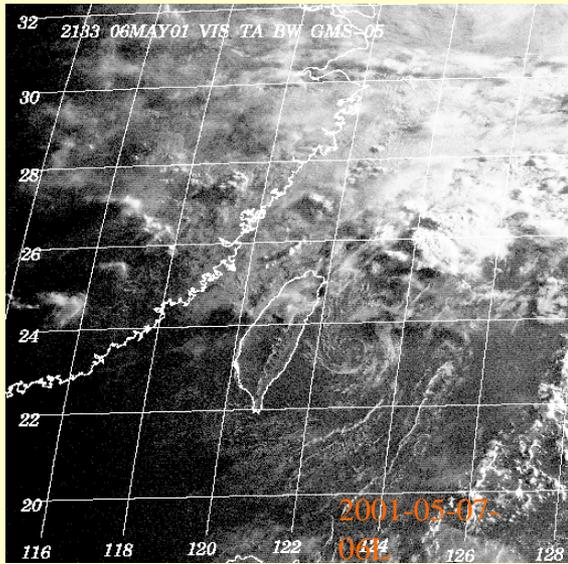
# 颱風海燕併入中緯度天氣系統轉化成溫帶氣旋

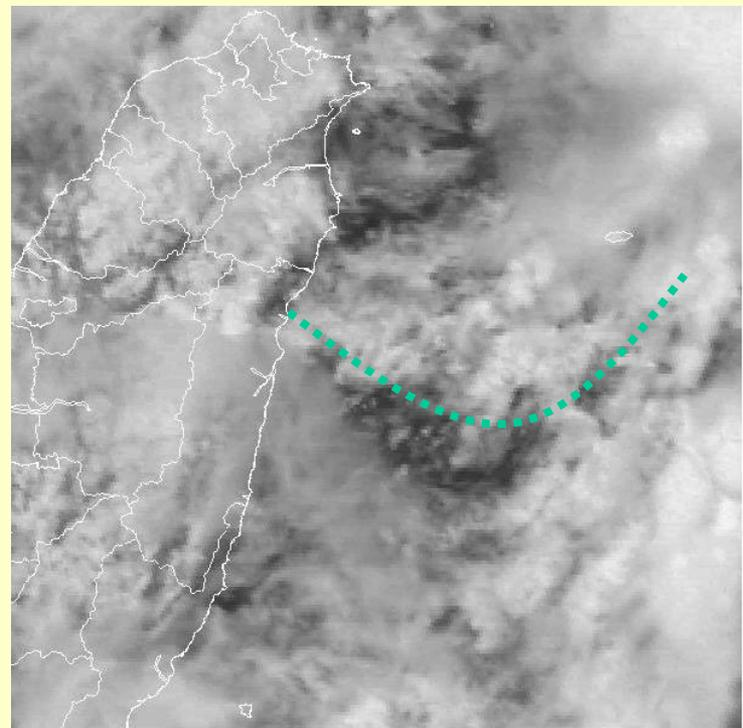
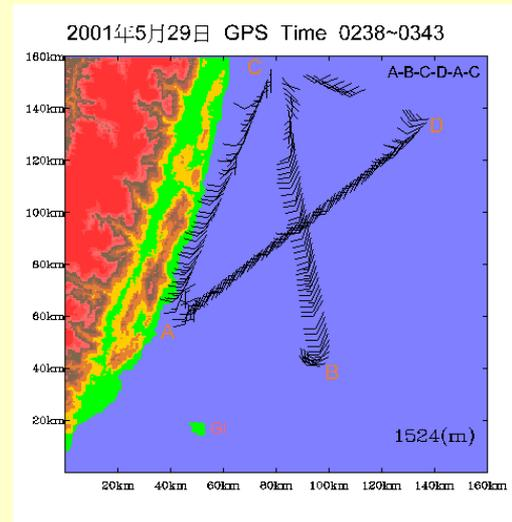
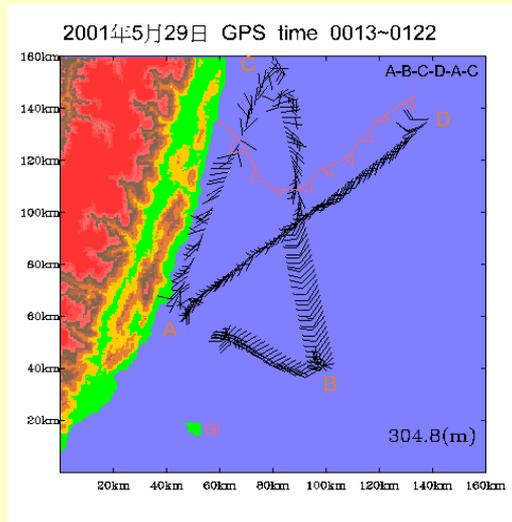
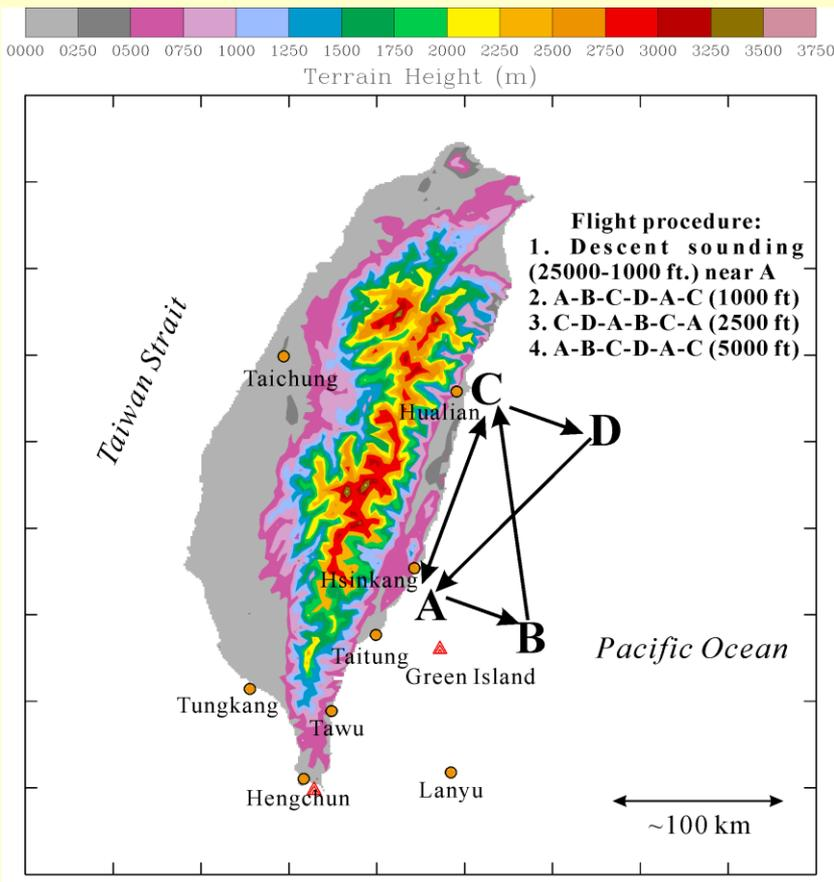
Typhoon 25W (Haiyan) was located in the East China Sea near 28.1N 128.5E at 12:00 UTC. Haiyan has been moving east-northeastward at 15 knots with maximum sustained winds estimated at 70 knots, gusts to 85 knots.

CREDIT: NOAA



# 綠島中尺度實驗(GIMEX)觀測之中尺度背風氣旋 May 7, 2001





綠島實驗漢翔航空支援之飛機飛行路徑示意圖。此時天氣型態為梅雨鋒面滯留花蓮南方外海呈東西走向，跨鋒方向不同高度之氣流特徵得以被實際觀測。注意鋒面上有許多正在發展中的雲系。

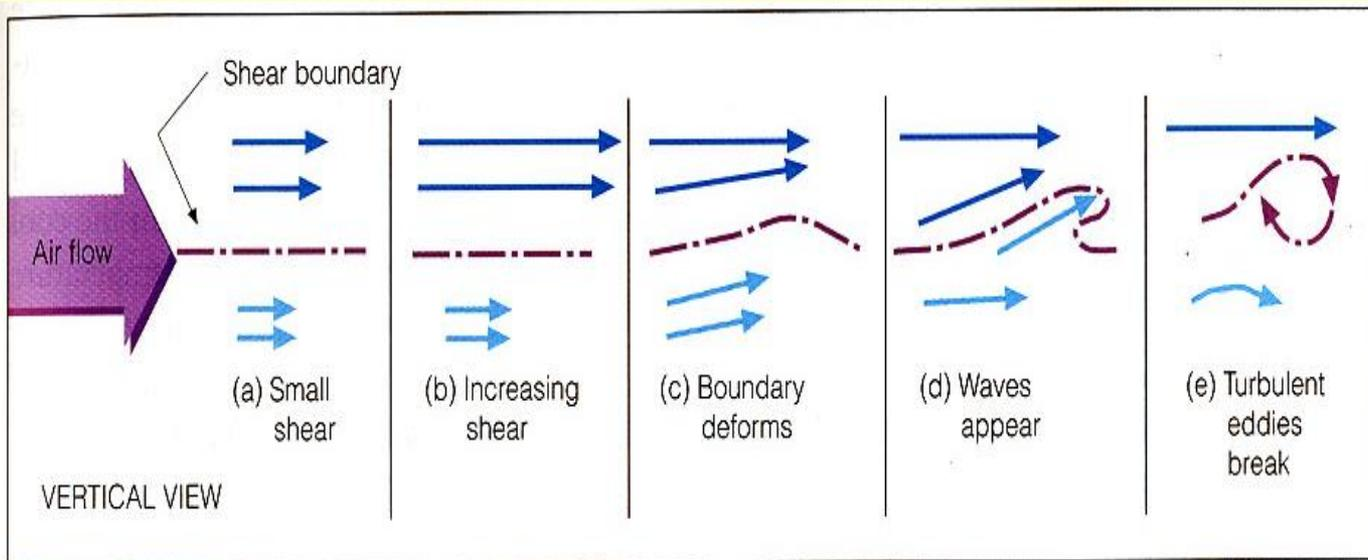


FIGURE 2

Turbulent eddies forming in a wind shear zone produce these clouds called billow clouds.

Billow  
clouds  
induced by  
wind shear

強風切帶內的擾動渦流造成之浪雲

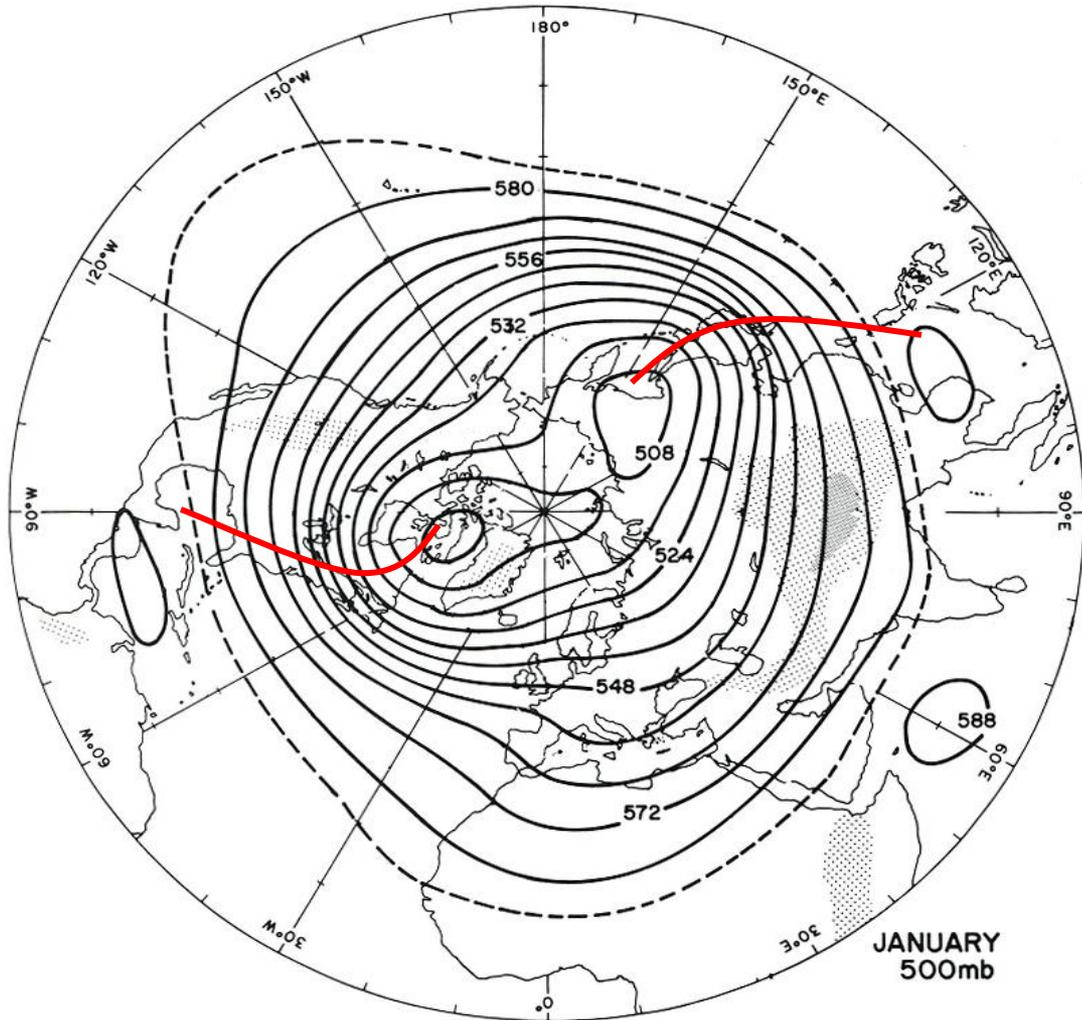


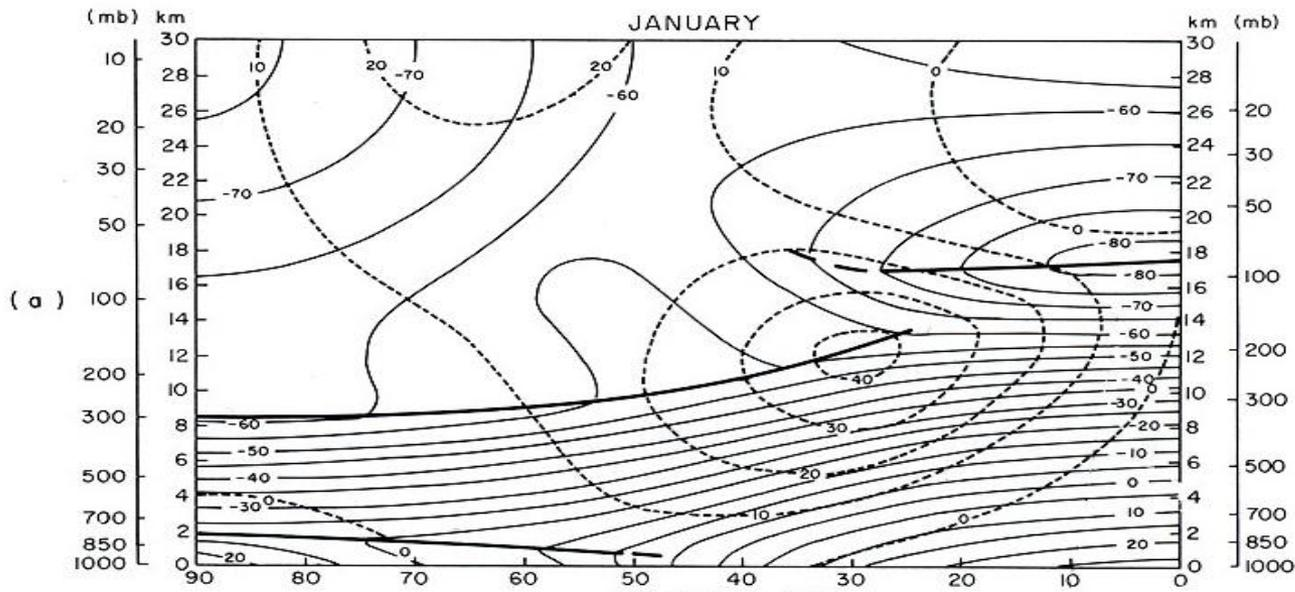
# 冬季500hPa平均重力位高度分布

行星尺度之大氣現象  
\*極渦與副熱帶高壓  
\*西風帶與西風擾動  
\*東亞與北美主槽

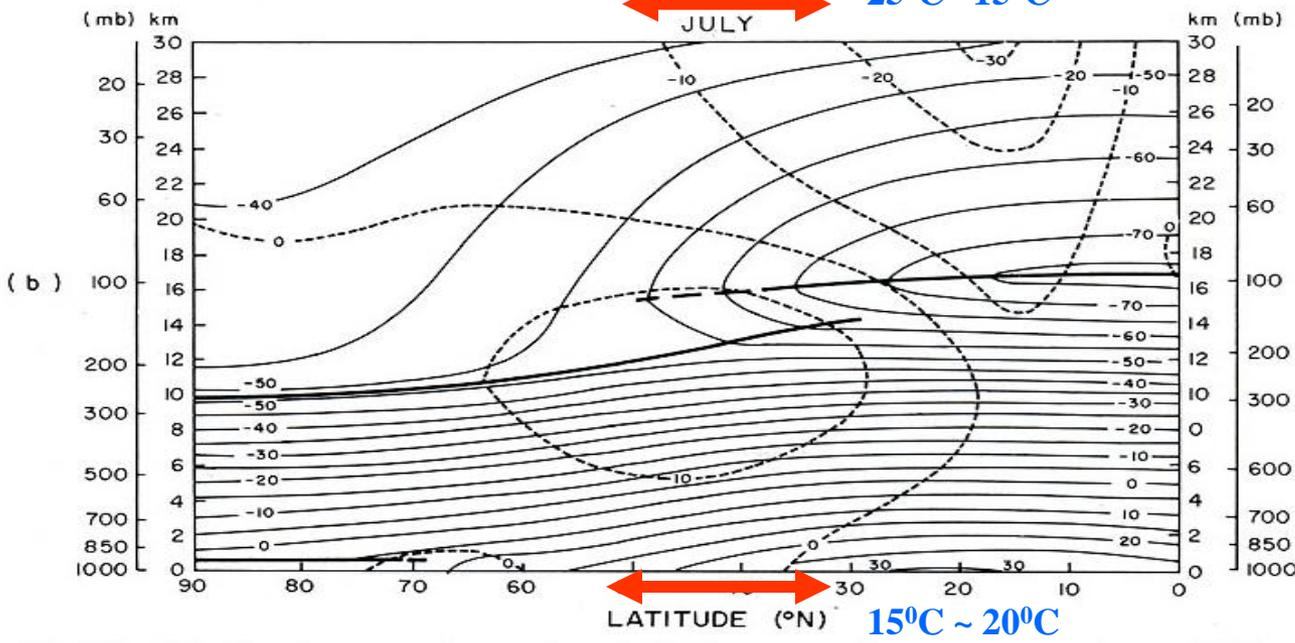
## 形成原因

\*海陸交界之不  
均加熱過程  
\*大陸地形對氣流  
之動力過程  
\*非線性動力過程





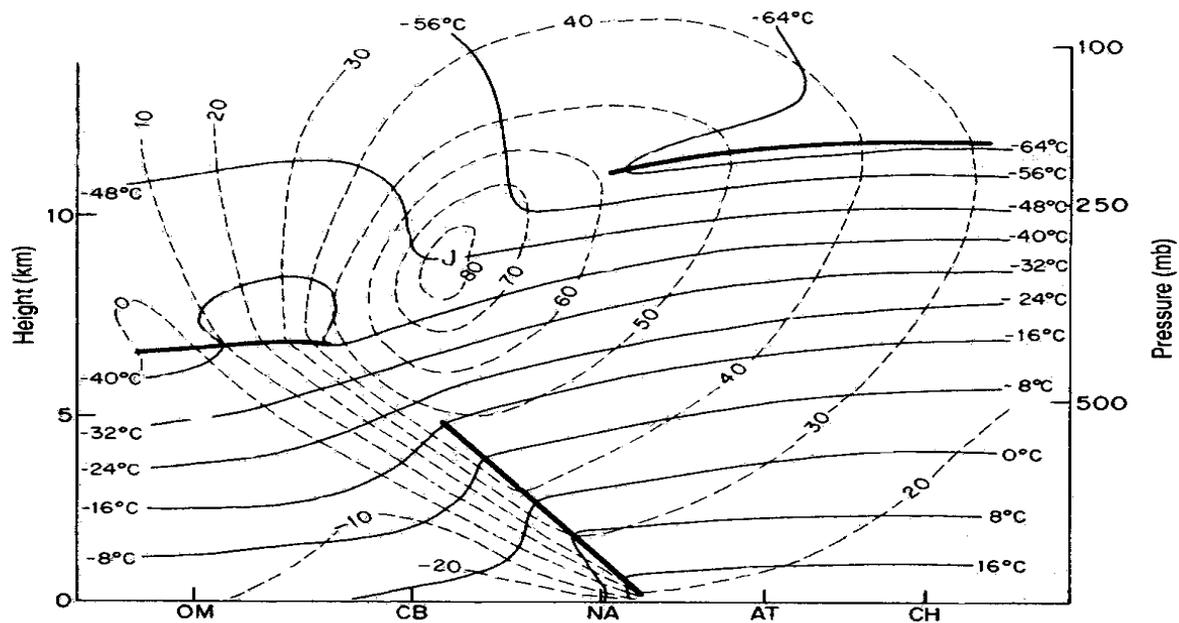
上圖：北半球一月緯向平均的溫度和緯向風的分布。



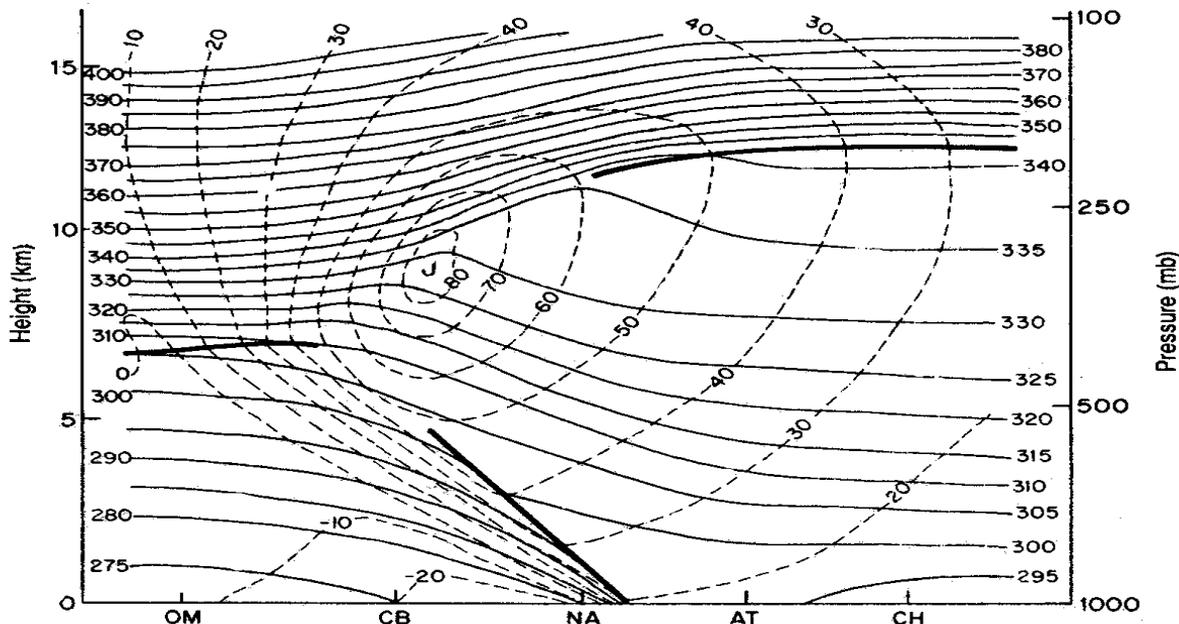
下圖：北半球七月緯向平均的溫度和緯向風分布。

水平溫度梯度及平均緯向風垂直風切兩者大小成正比

Fig. 1.11 Meridional cross sections of longitudinally averaged temperature in degrees Celsius (—) and zonal wind in meters per second (---) for the northern hemisphere in January (a) and July (b). Positive zonal winds indicate flow from west to east. Heavy lines denote the tropopause and the Arctic inversion. (After *Arctic Forecast Guide*, U.S. Navy Weather Research Facility, 1962.)



(a)



(b)

冷鋒通過時大氣溫度（上圖）及位溫（下圖）與緯向風的垂直剖面 注意此時西風噴流強度遠超過平均值

位溫：

$$R/C_p$$

$$\Theta = T ( 1000/P )$$

在壓力為P,溫度為T的一乾空氣塊,若經由乾絕熱膨脹(或壓縮)過程,使其壓力達到1000hpa,此空氣塊所具有的溫度,稱之位溫(potential temperature)。

任何一空氣塊都有其唯一的位溫值,此位溫值在空氣塊經由乾絕熱過程時,具保守性質。

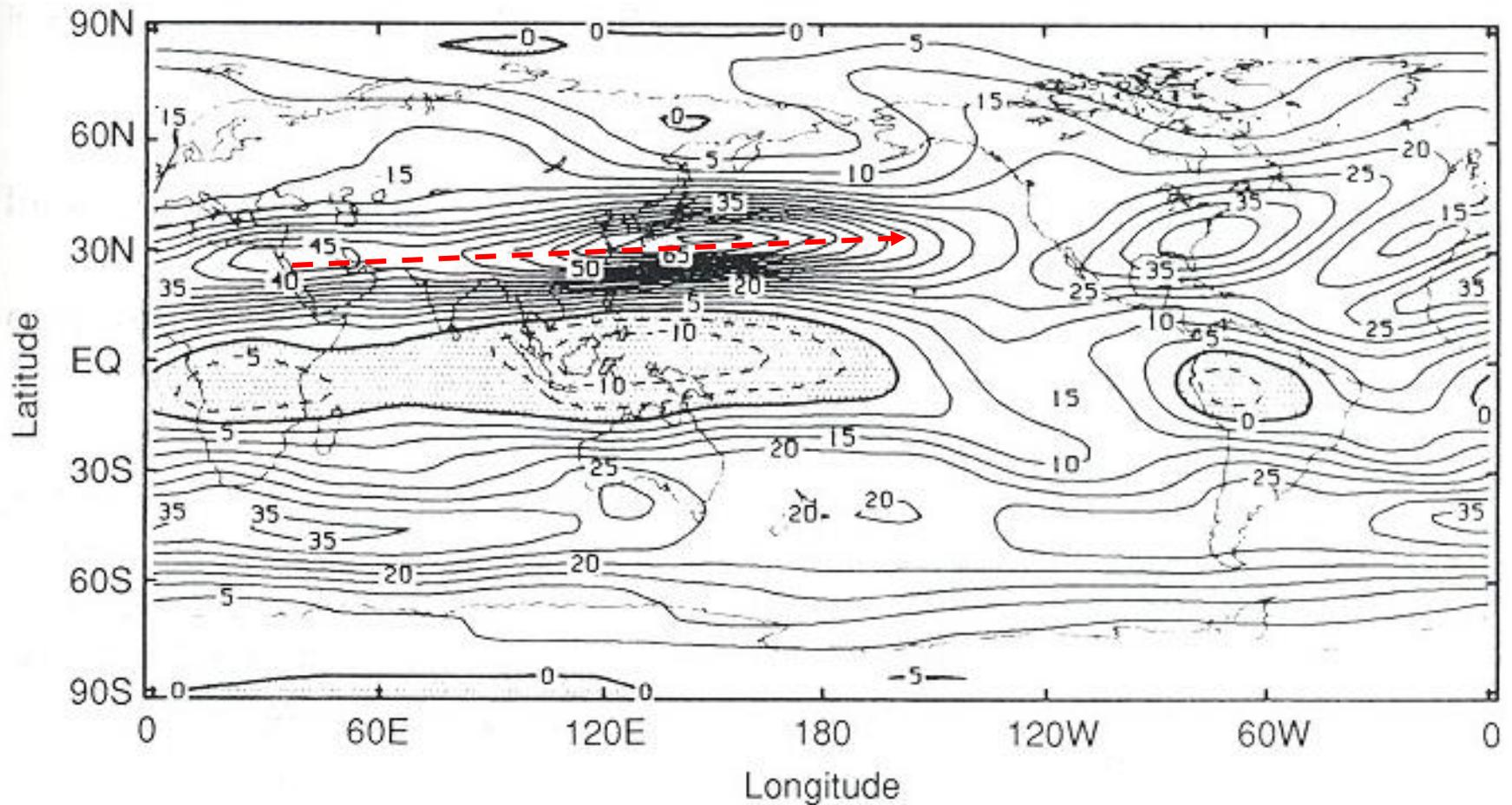
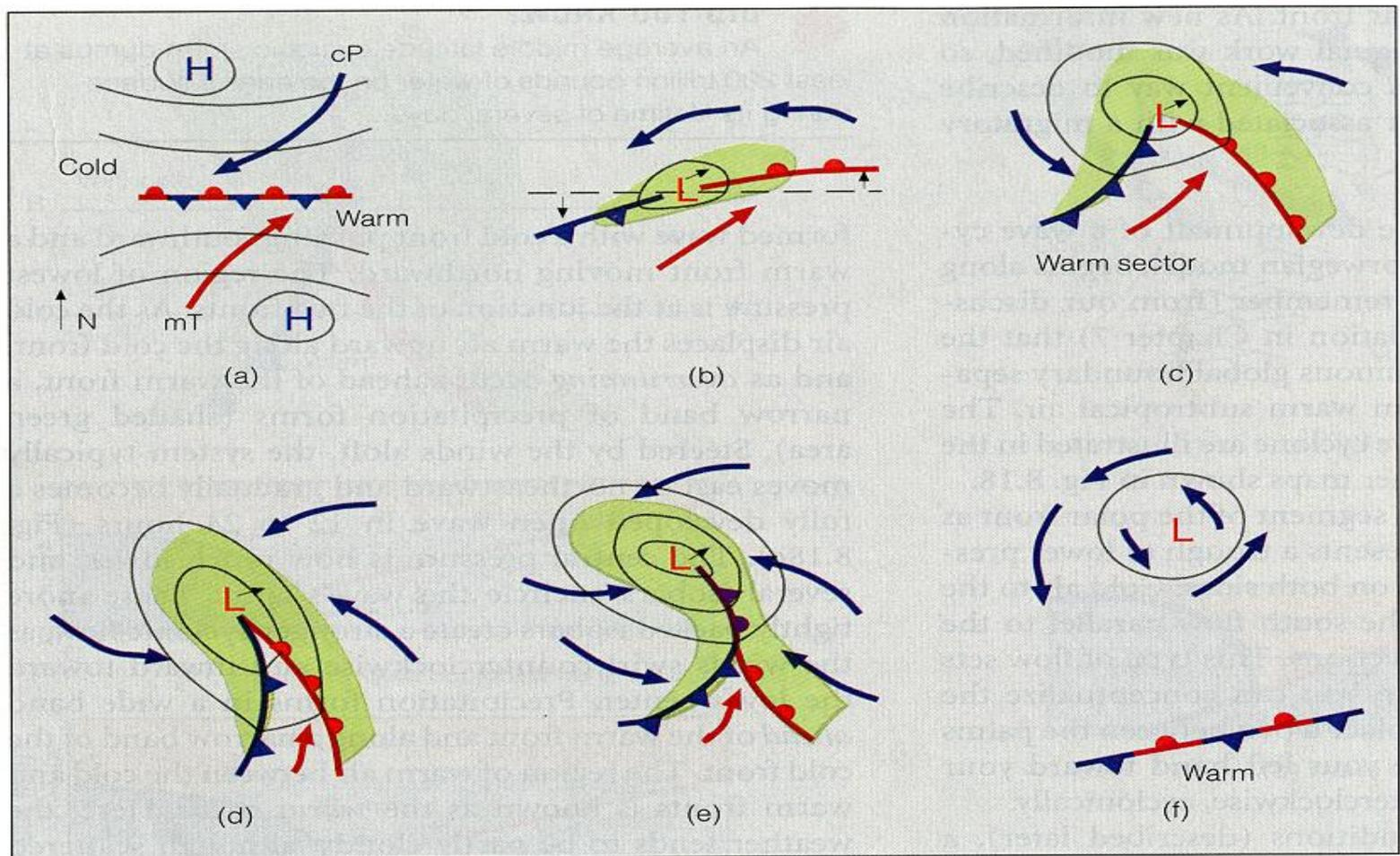
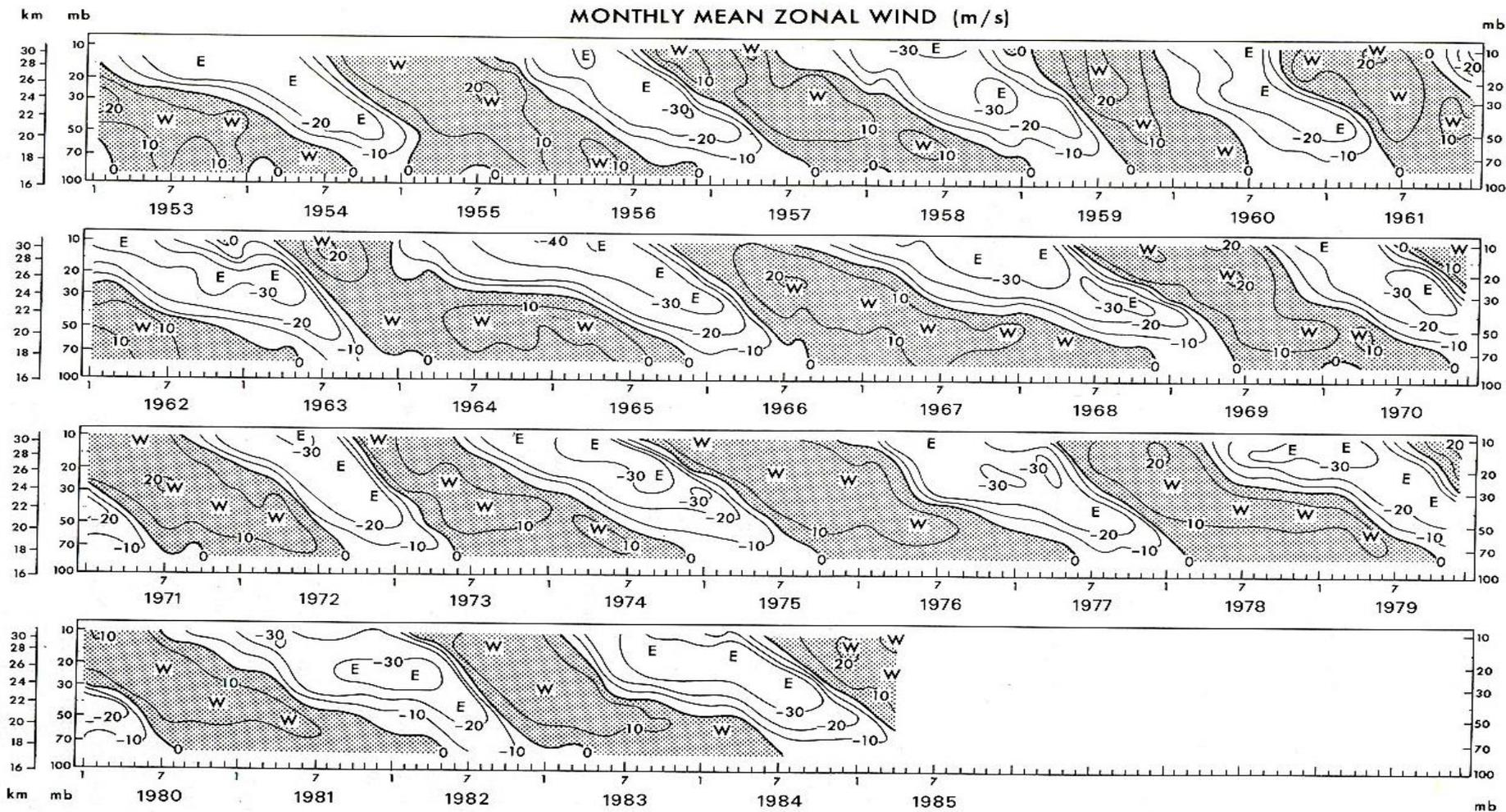


Fig. 6.2 Latitude-longitude cross section of time-averaged zonal wind speed at 200 mb for DJF averaged for years 1980-1987. (After Schubert *et al.*, 1990.)

1980-1987年12-1-2月200mb時間平均緯向風速分佈。  
 (噴射氣流之空間分布)

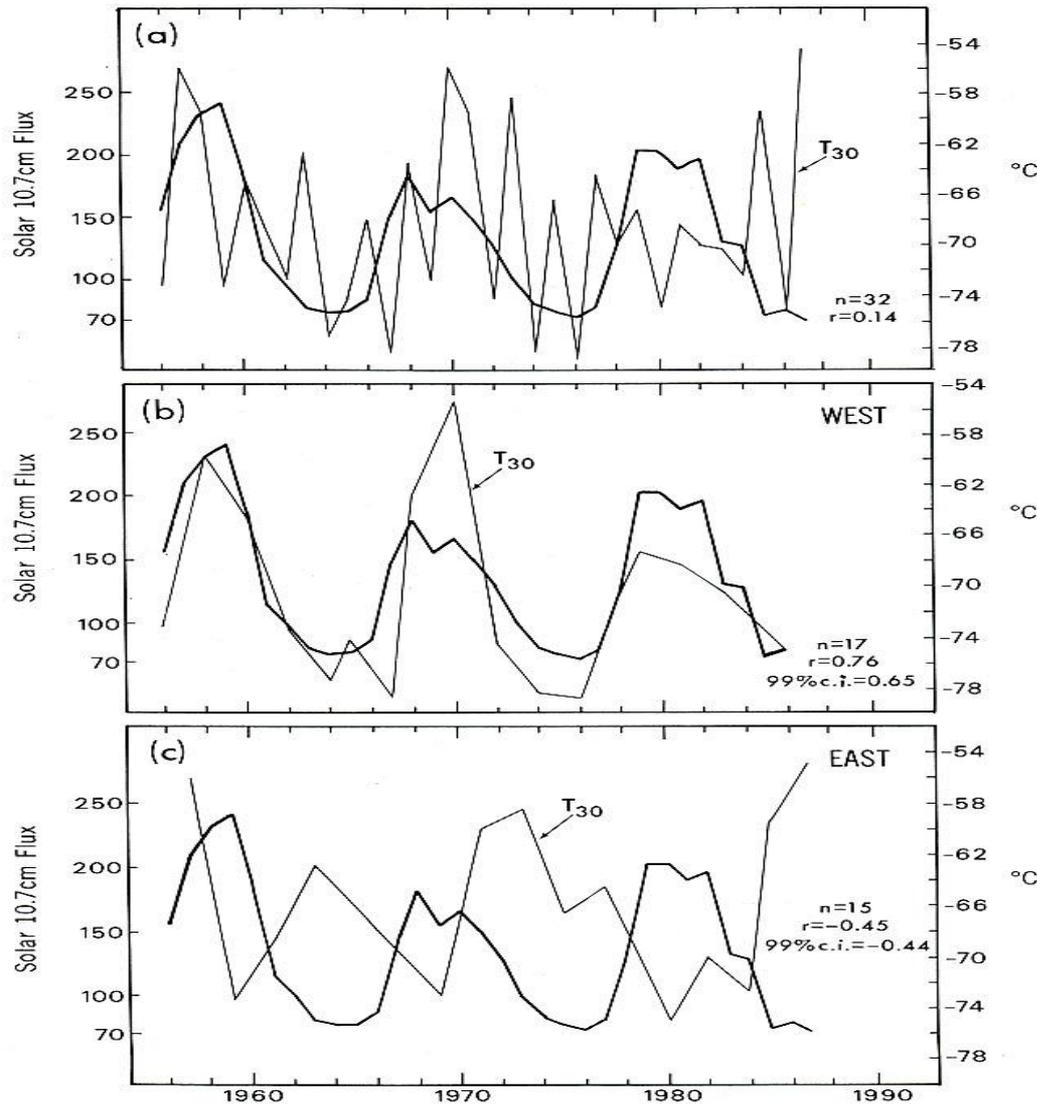
根據極鋒理論在北半球一理想氣旋的生命週期。在其生命期中，此系統因動力因素向東移。字母L旁的小箭頭表示風暴的移動方向





**FIGURE 16.1.** Time-height section of the monthly-mean zonal wind component near the equator in  $\text{m s}^{-1}$ , showing the QBO signal of alternating westerly and easterly winds. The section is based on data from Canton Island ( $3^{\circ}\text{S}$ ,  $172^{\circ}\text{W}$ ; 1953–1967), Gan ( $1^{\circ}\text{S}$ ,  $73^{\circ}\text{E}$ ; 1967–1975), and Singapore ( $1^{\circ}\text{N}$ ,  $104^{\circ}\text{E}$ ; 1976–1985) (after Naujokat, 1986).

接近赤道區的月平均緯向風之時間高度分布圖。準兩年振盪清晰可見。



10.7cm太陽通量的時間序列(粗線，單位： $10^{-22} \text{ W m}^{-2} \text{ Hz}^{-1}$ )及北極冬季平均30mb高度的溫度

(a)1956-1987年32個冬天

(b)17個QBO西風為主的冬天

(c)15個QBO東風為主的冬天

太陽變動與地球大氣的關係

**FIGURE 16.2.** Time series of the 10.7-cm solar flux (thick solid lines) in units of  $10^{-22} \text{ W m}^{-2} \text{ Hz}^{-1}$ . Thin solid lines show the mean 30-mb temperature in  $^{\circ}\text{C}$  at the North Pole for all 32 winters from 1956 through 1987 (a), for 17 winters in the west phase ( $\bar{u} > 0$ ) of the QBO (b), and for 15 winters in the east phase ( $\bar{u} < 0$ ) of the QBO (c). Winter conditions are taken as the average of the months of January and February. The number of winters  $n$ , the correlation coefficient  $r$  between the solar flux and the 30-mb winter temperature, and the 99% confidence level are shown on the right in each figure (after Labitzke and van Loon, 1988).



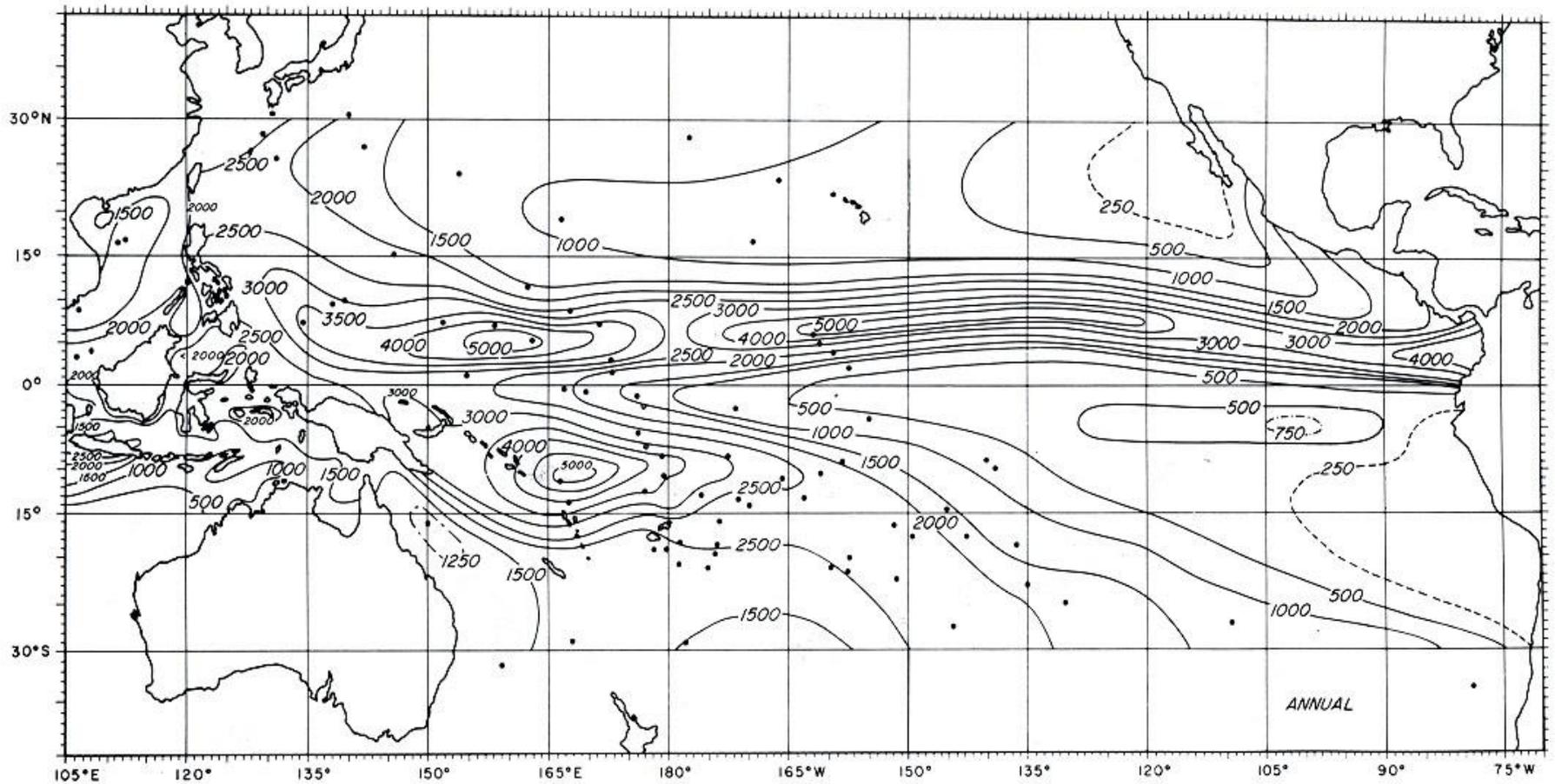
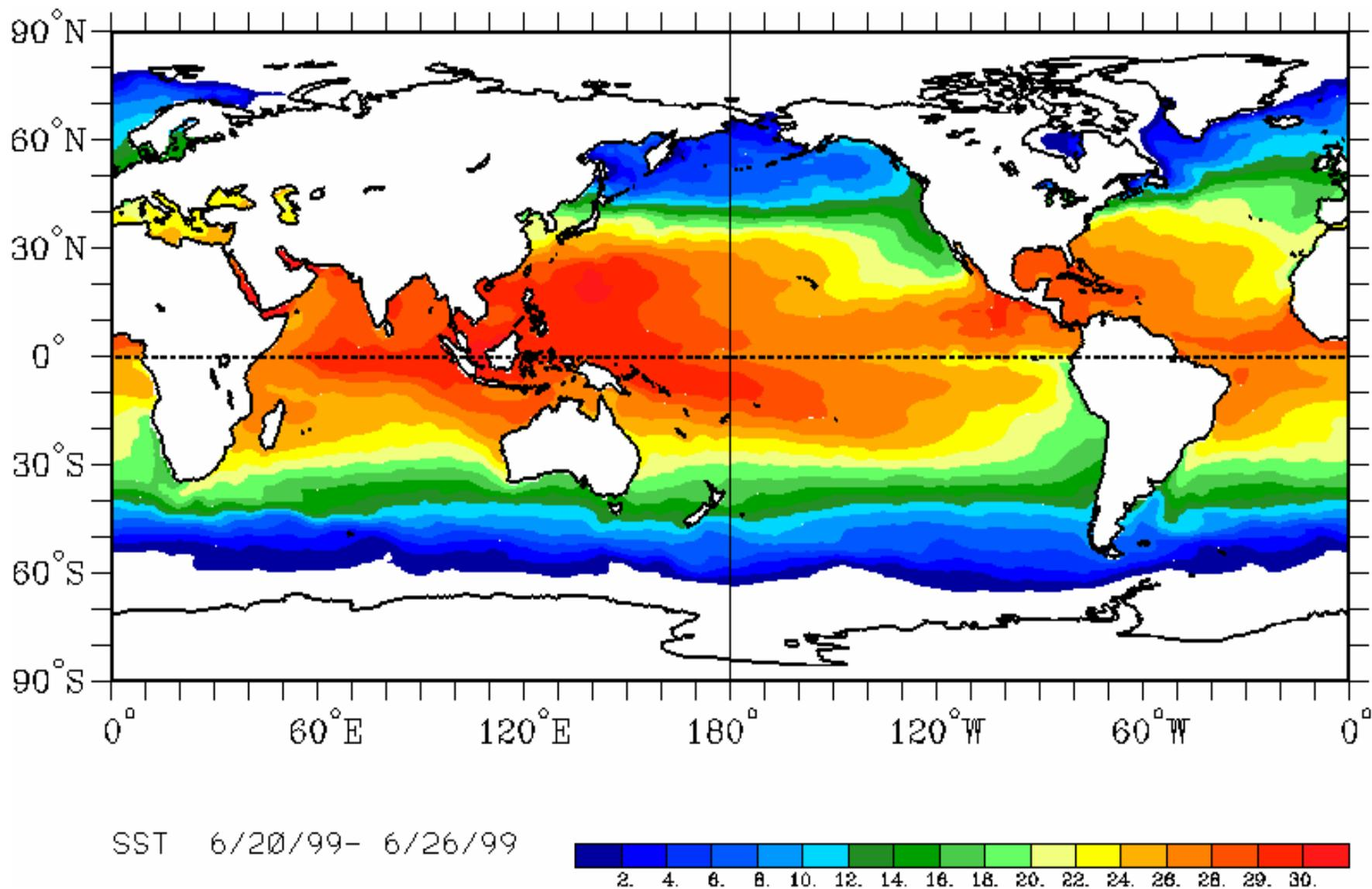


**Fig. 1.20** Average annual precipitation (in millimeters) over the tropical Pacific Ocean. Dots represent stations used in the analysis. (After R. C. Taylor, *An Atlas of Pacific Islands Rainfall*, Hawaii Institute of Geophysics, 1973.)

熱帶太平洋平均年降水分布。



1999年6月20-26日平均海面溫度。

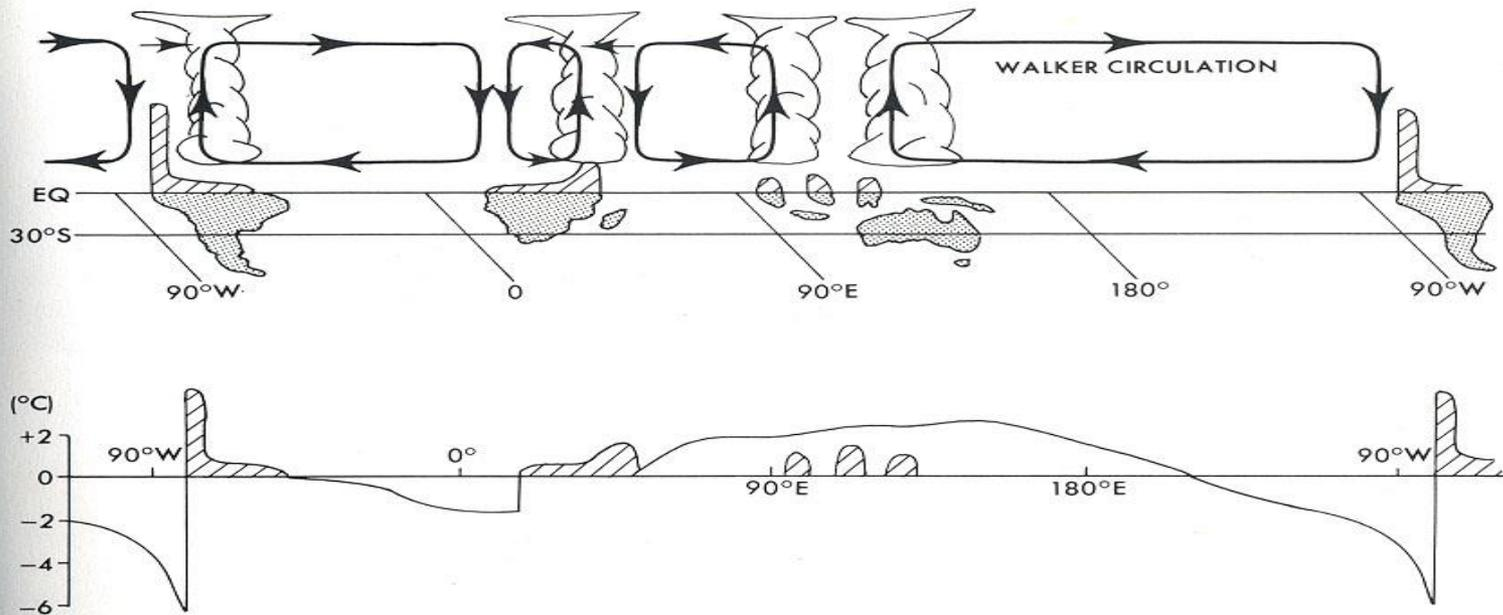
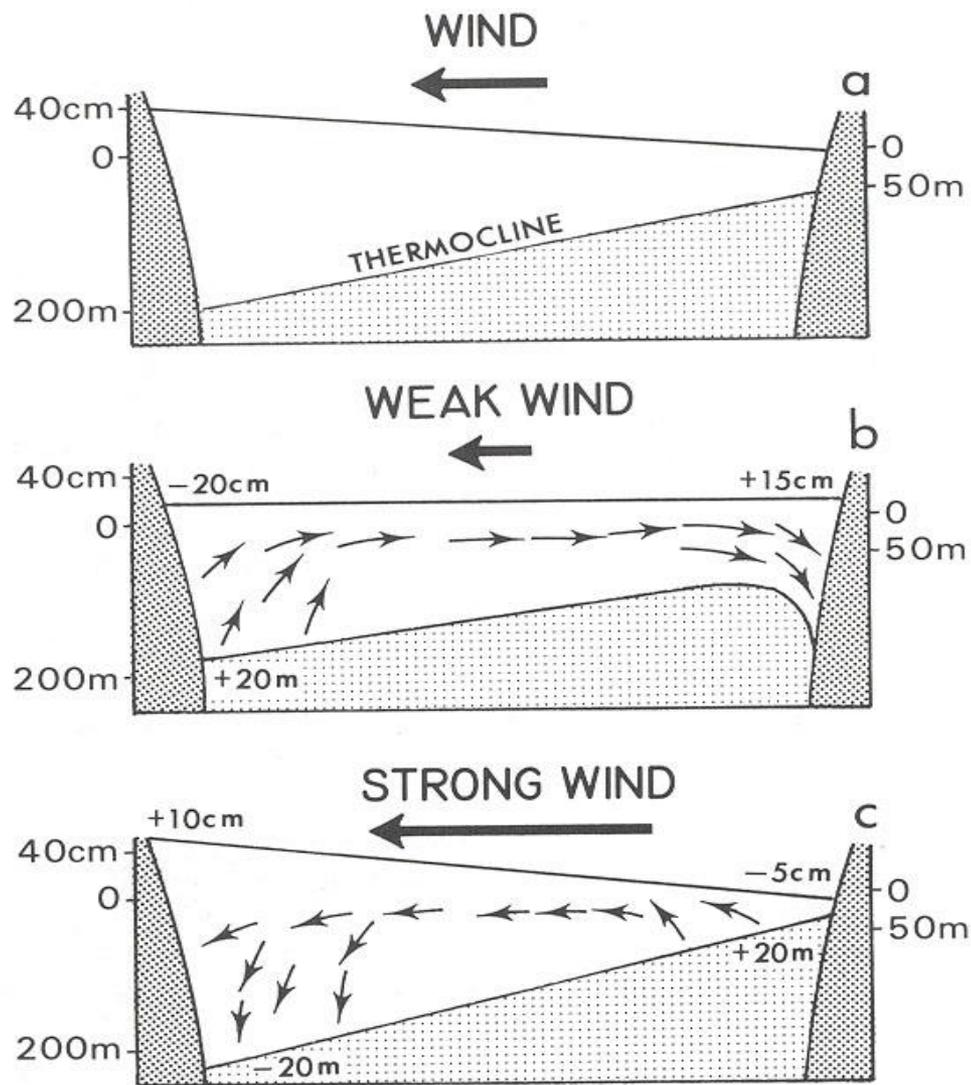


**FIGURE 16.5.** Schematic diagram of the normal Walker circulation along the equator during non-ENSO conditions. Rising air and heavy rains tend to occur over Indonesia and the western Pacific, southeast Africa, and the Amazon area in South America, while sinking air and desert conditions prevail over the eastern equatorial Pacific and southwest Africa (see also Fig. 7.24). The strongest branch of the Walker circulation over the Pacific is related to the very warm SST in the west Pacific where the air is rising, and the cool SST in the east Pacific where the air is sinking. The SST departures from the zonal-mean along the equator are shown in the lower part of the figure (after Wyrtki, 1982).

在非聖嬰條件下沿赤道，一般沃克環流的概要分布：在印尼、西太平洋、東南非洲、南美亞馬遜地區有上升空氣和豪雨，而在東赤道太平洋、西南非洲有下沉運動及較乾的現象，下圖為海面溫度的相對分布。



因地面風的改變所造成赤道太平洋熱力結構的改變。

(a)一般東信風吹送之下，海面向西上升 斜溫層變厚。

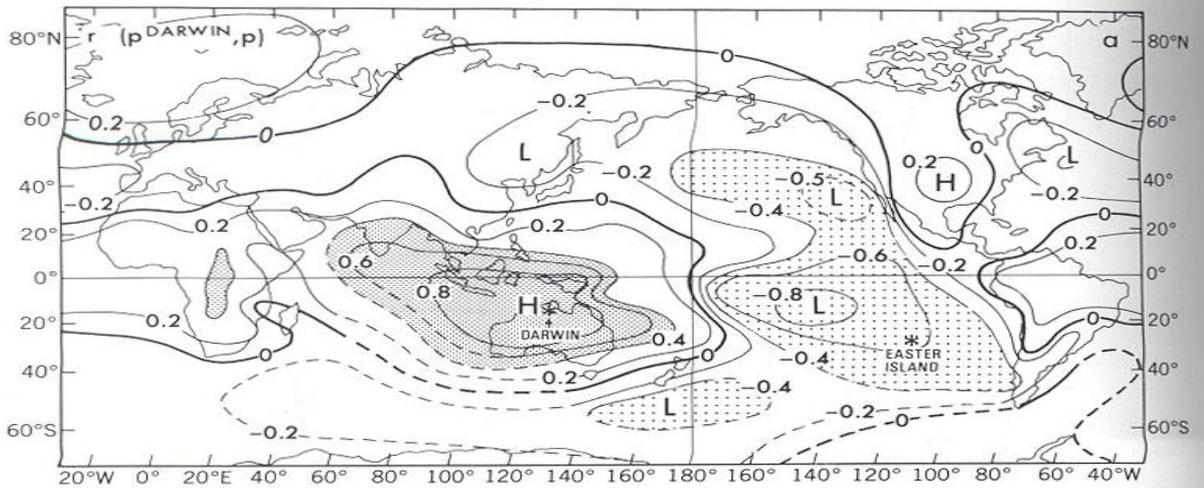
(b)當東風變弱，海水面向西傳送，接近南美海岸斜溫層變厚，湧升流被抑制。

(c)信風很強的情形，湧升流被加強。

**FIGURE 16.7.** Response of the thermal structure of the equatorial Pacific to changes in the surface winds. (a) Under normal easterly trade wind conditions sea level rises to the west and the thermocline deepens. (b) When the winds relax, water sloshes east, which leads to a rise in sea level and a deepening of the thermocline near the South American coast. In the western Pacific, sea level drops and the thermocline rises (El Niño conditions). (c) The normal situation is amplified during strong trade winds [anti-El Niño or La Niña conditions (after Wyrtki, 1982)].

# 大氣海洋交互作用

上圖：年平均海平面氣壓距平和澳洲達爾文氣壓距平的相關係數分布。可表示大氣質量在聖嬰現象發生時的全球傳送。



下圖：澳洲達爾文氣壓距平和海面溫度距平(1950-1979年)的相關係數分布。

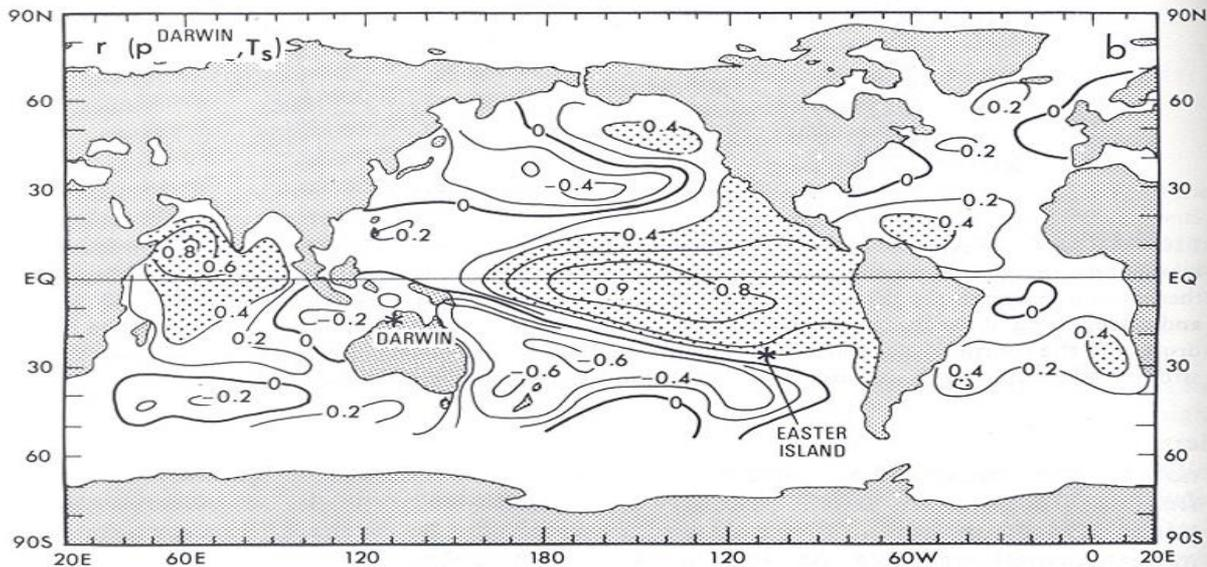


**FIGURE 16.8.** (a) Horizontal distribution of the correlation coefficient between annual-mean sea level pressure anomalies over the globe and the corresponding pressure anomalies in Darwin, Australia (12°S, 131°E) as a measure of the Southern Oscillation. The map shows that global shifts of atmospheric mass take place during ENSO episodes (adapted from Trenberth and Shea, 1987). (b) Horizontal distribution of the correlation coefficient between annual-mean sea level pressure anomalies in Darwin and sea surface temperature anomalies over the globe for the 30-year period 1950–1979. Areas with anomalies greater than 0.4 are stippled.

# 大氣運動的能量來源,不均勻加熱旋轉環實驗,地球大氣能量平衡與分佈,大氣環流的動能循環

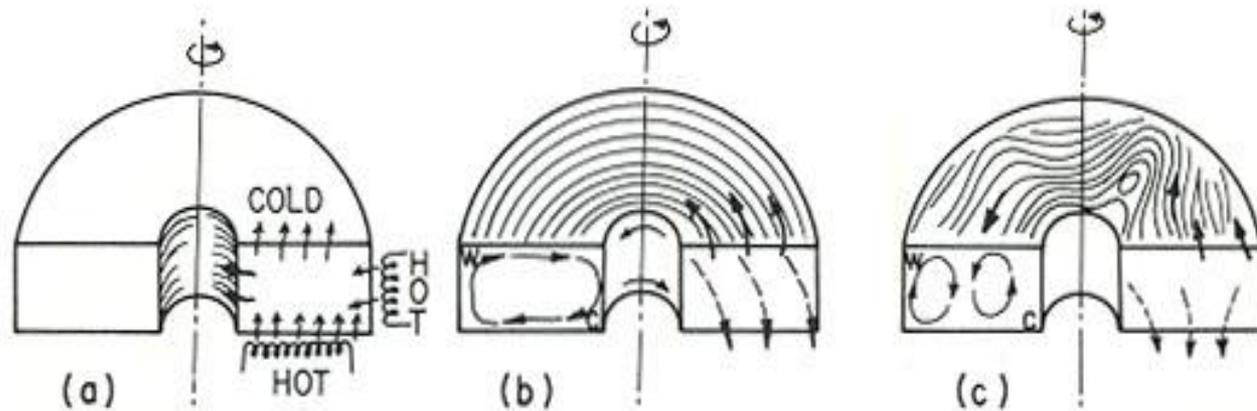


**Fig. 9.10** A differentially heated rotating annulus experiment. (a) The distribution of heating and cooling. (b) Symmetric regime showing the “Hadley circulation” (cross section at left) and the azimuthal flow relative to the rotating annulus (inner wall and cross section at right). Note that the azimuthal flow varies with height. (c) The wave or “Rossby” regime. Cross section at left shows azimuthally averaged radial and vertical circulation. Arrows at top and right indicate flow relative to the rotating annulus. Note that the flow varies with azimuth angle and with height and that the radial component may be very large locally.

旋轉環不均勻加熱實驗：(a)加熱和冷卻的分布；(b)哈德里胞的示意圖；(c)羅士培波的示意圖

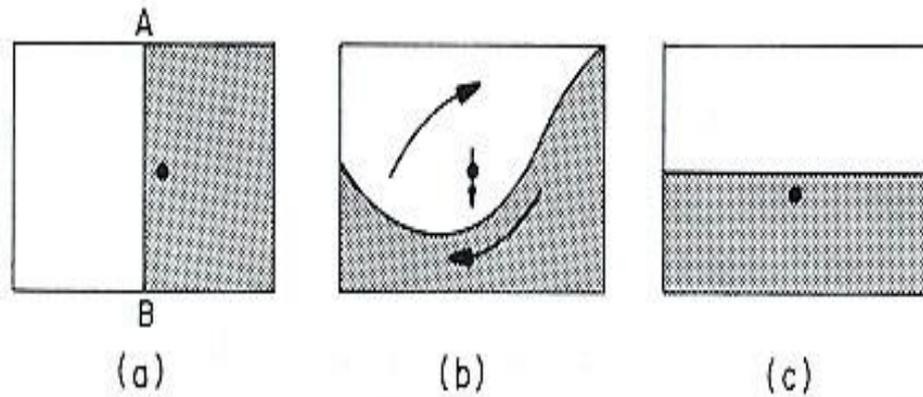


Fig. 9.1 (a) Heavier (shaded) and lighter fluids separated by a movable partition AB. The dot represents the center of gravity of the two-fluid system. (b) Fluids in motion following the removal of the partition. (c) Equilibrium configuration of the fluids after the motion has been dissipated by friction.

(a)較輕和較重的流體被一可移除的隔板所分隔，黑點為兩流體的重心

(b)隔板移除後，流體的移動

(c)平衡狀態

\*位能轉換成動能再回歸穩定狀態的過程。

\*地球大氣位能的形成主要來自太陽加熱。

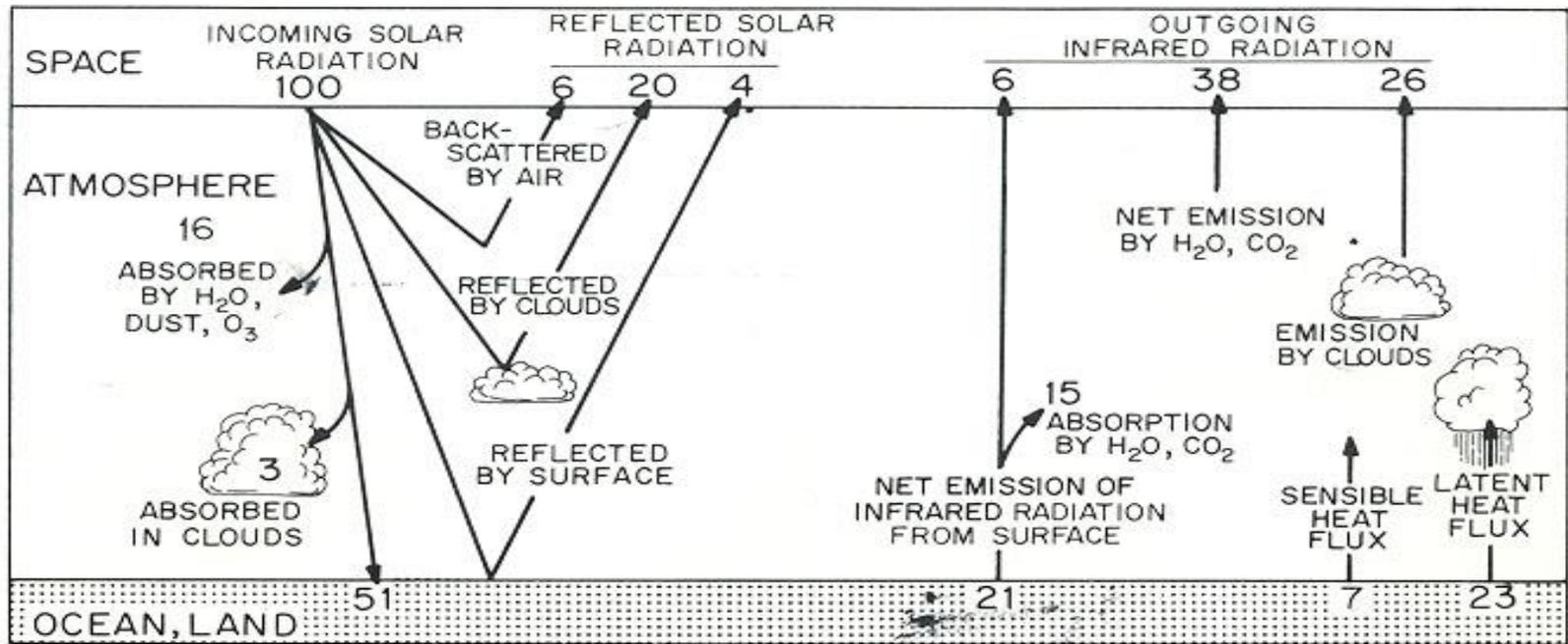


**Fig. 7.1** The annual mean global energy balance for the earth-atmosphere system. (Numbers are given as percentages of the globally averaged solar irradiance incident upon the top of the atmosphere.) See text for further explanation. [Adapted from "Understanding Climatic Change," U.S. National Academy of Sciences, Washington, D.C. (1975), p. 14, and used with permission.]

地球大氣系統的年平均全球能量平衡。  
 太陽輻射、大地輻射、雲、大氣—地面—海洋之交互作用。

# 大氣運動的能量循環

